

European Commission



Semi-Rigid Behaviour of Civil Engineering Structural
Connections

COST C1

REPORT OF WORKING GROUP 6 - NUMERICAL
SIMULATION

**NUMERICAL SIMULATION OF SEMI-RIGID
CONNECTIONS BY THE
FINITE ELEMENT METHOD**

Edited By
Kuldeep S. Viridi
City University London

Brussels Luxembourg 1999

PREFACE

This document has been prepared by Working Group WG6 - Numerical Simulation, of the COST-C1 project on the Control of Semi-Rigid Behaviour of Semi-Rigid Connections in Civil Engineering Structures. The activities of COST-C1 were organised through 7 Working Groups.

| | |
|---------------------|--|
| Working Group WG1 - | Concrete connections |
| Working Group WG2 - | Steel, Composite and Column Base connections |
| Working Group WG3 - | Timber connections |
| Working Group WG4 - | Database |
| Working Group WG5 - | Seismic Action |
| Working Group WG6 - | Numerical Simulation |
| Working Group WG7 - | Polymeric connections |

The brief of the Working Group 6 was to establish guidelines for the numerical simulation by the Finite Element method of the behaviour of semi-rigid connections of all types : concrete, steel, composite, timber, polymeric, etc. The Working Group has had a membership of some 30 research establishments across Europe. Much of the activities of the Working Group 6 were based on exchange of experience gained in carrying out numerical studies on the full range of connections. The Working Group met on 10 occasions at meetings hosted by a number of the member institutions, and some 50 working documents were prepared. Many of these have been published in the three events organised by COST-C1, at Strasbourg (1992), Prague (1994), and Liège (1998), as well as in many other conferences and journals. The aim of this publication is to present the key findings in the course of the project, supplemented by typical applications to specific connection types. It also emerged during the various studies that for reliable comparisons, there existed the need for some very carefully conducted experiments. The final chapter of the book describes the tests carried out for this purpose by the team from Bundeswehr Universität München.

The editor would like to acknowledge the contributions of all the members of the Working Group.

CONTENTS

| | | |
|------------|--|-------|
| Preface | | (iii) |
| Chapter 1 | Numerical Simulation of Semi-Rigid Connections By the Finite Element method | 1 |
| Chapter 2 | Numerical Aspects of the Simulation of End-Plate Connections | 13 |
| Chapter 3 | Column Base Connections | 32 |
| Chapter 4 | Guidelines for the Numerical Modelling of Beam-to-Column Minor Axis Joints | 48 |
| Chapter 5 | Benchmark Experiments for Numerical Simulation of T-Stubs | 61 |
| Appendix 1 | Contact addresses of the authors | 71 |

GUIDANCE ON GOOD PRACTICE IN SIMULATION OF SEMI-RIGID CONNECTIONS BY THE FINITE ELEMENT METHOD

K. S. Viridi

Structures Research Centre, City University, London EC1V 0HB, UK
Chairman, COST C1 Working Group WG6 on Numerical Simulation

Check Last

ABSTRACT: The objective set for Working Group 6 on Numerical Simulation was to complement the experimental investigations with computations aimed at improving the understanding of the basic phenomena involved. The analytical tool adopted is the Finite Element Method. Considerations of material non-linearity, including yielding of steel, cracking and crushing of concrete, and splitting of timber, become essential. Other aspects to consider include contact and friction between surfaces. Some other parameters to consider relate to the method itself - mesh size and choice of element formulation. The work of the group has helped to gain some useful experiences in the numerical simulation of the connection behaviour.

1 INTRODUCTION

The potential benefits of using semi-rigid connections in structural frames are well recognised. Indeed, the Eurocode for the design of steel structures (Eurocode 3 [1]) has extensive coverage of the topic. However, designers at large have not as yet adopted such designs on a wide basis. Partly, this stems from a lack of understanding of the behaviours of semi-rigid joints. Perceiving this, a number of research groups across Europe launched a concerted programme of collaboration under the COST-C1 project – *Control of the Behaviour of Semi-Rigid Connections in Civil Engineering*. The project covers all types of connections - steel, composite, column bases, concrete, timber and polymeric.

The variety of materials and of structural forms used makes it nearly impossible to propose a single theory to describe the behaviour of all connections. That is the principal reason why much of the work under COST-C1 was organised under four of the materials oriented working groups on concrete, steel and composite, timber and polymeric connections. Within those groups, research effort was spent in conducting co-ordinated sets of experiments to study the behaviour of connections. Experiments are, however, expensive. The variety of structural forms used and the combinations of parameters that influence the behaviour of connections being so large, it is also nearly impossible to conduct the required number of definitive sets of experiments which would help in understanding the behaviour fully.

Since computing power is becoming increasingly affordable, numerical simulation has been seen as an inexpensive alternative to physical experiments. Thus, the key term of reference of the Numerical Simulation Working Group (WG6) was to attempt to simulate the behaviour of connections numerically, leading the way towards "numerical experiments".

The principal tool available for numerical simulation is the Finite Element method. This method of analysis allows complex geometry to be modelled fairly accurately. Material non-linearity such as plasticity in metals and cracking in brittle materials can be adequately considered. Complex loading arrangements and boundary conditions can also be reasonably simulated. Most standard programs now available have provisions for dealing with difficult aspects such as contact, gap and friction.

While many commercial packages available attempt to include all the above aspects, the actual theoretical techniques used by these programs are, however, often different. Notwithstanding the many facilities offered by commercial Finite Element packages, an attempt to analyse the behaviour of a given connection nearly always leads to difficult decisions for the analyst as to how precisely to model different aspects involved. Recognising these difficulties, the Numerical Simulation Working Group (WG6) was formed to include researchers working with connections in all materials, so that the experience gained by one team in the analysis of connections in one material could be shared by teams working with different materials, but perhaps involving common phenomenon.

The activities of COST-C1 Working Group have been presented at three major events – the Strasbourg Workshop (1992) [2], Prague Workshop (1994) [3] and the valedictory Liège Conference (1998) [4]. This document is aimed at presenting information, much of it not included elsewhere in COST publications, which could be useful for researchers aiming to study the behaviour of connections using the Finite Element approach.

2 MODELLING WITH FINITE ELEMENTS

There are several packages, which are commercially licensed to enable linear or non-linear analysis to be carried out. The COST-C1 Numerical Simulation Working Group has made no attempt to compare one package against another. The aim has been to arrive at certain principles of good practice.

When applying finite elements for studies of this nature, decisions of need to be made on several aspects of modelling the real behaviour. These include representation of geometry, constitutive laws, boundary conditions, and loading. In the context of simulation of connection behaviour up to failure, it is understood that non-linear rather than a linear analysis will be used.

2.1 Geometry

The principal aim of idealising a structure (or a component such as a connection) when using the Finite Element Method is not necessarily to achieve an accurate representation of the geometry. Since the aim really is to achieve a sufficiently accurate representation of the *behaviour* of the structure under the applied loading, emphasis needs to be placed on simulating the whole system. While modern FE packages offer powerful pre-processors to assist with modelling of the geometry and meshes rather conveniently, the decisions can best be made with an awareness of the underlying theory. Experience with a package improves the chances of obtaining satisfactory results.

2-D versus 3-D Modelling

Intuitively, the first question to ask is whether the connection can be modelled as a 2-D structure? If successful, there is the payback of simplicity and a faster turnaround time in terms of setting up of the numerical model and the processing of results. However, a careful look at the behaviour of most connections reveals that 2-D modelling is generally not satisfactory. Hence, 3-D modelling is recommended for studying all types of connections, especially if the object is to obtain the full response up to collapse.

Choice of Elements

Commercial Finite Element programs offer a wide range of elements. In modelling steel connections, the choice is between solid elements or shell elements. While the latter appear to serve adequately when dealing with the mechanisms that develop in plate components of beams and column being connected, they generally prove inadequate when interfacing with other components of a connection, particularly with bolts. Even when adopting solid elements, there is the choice between the simple 8-noded brick element and the more versatile 20 noded brick element. On the whole the 20 noded element gives better results, but the 8-noded element allows easier modelling of changes in shape such as fillets. Ten noded tetrahedral elements have also been found to give good results.

2.2 Material Properties

Elastic analysis will seldom suffice to represent the behaviour of connections for the full range up to collapse. The type of non-linearity required depends on the materials involved in the connection. Thus, plasticity is the main non-linearity required for steel components.

2.3 Steel

Plasticity

Plasticity is handled in FE programs through the device of separating the elastic and plastic strains from the total inelastic strain. In a perfectly elastic-plastic material, once the yield stress has been reached, no further increase in stress can take place for further increase in strain. The material is then said to *flow*.

The general approach adopted in FE packages is to model plasticity with strain hardening. In this case, beyond the yield stress, the stress continues to increase with increasing strains, but with a significantly reduced modulus of elasticity.

In a uniaxial state of stress, plasticity is easily visualised. However, in a multi-axial state of stress, criteria need to be defined so as to establish when yielding is likely to occur, and also to define the relationship between stresses and strains beyond the onset of yield. It is customary to use the von Mises yield criterion [5] for steel. In simple terms, the criterion states that yielding depends on a single scalar function which is itself a function of the stress invariants for an isotropic material.

Beyond the onset of yielding, for a perfectly plastic material, there is no change in the yield surface, and hence additional strains can only occur so as to ensure that the stress state lies on

the yield surface. For a strain hardening material, various options are available. In the *isotropic hardening material*, the yield surface changes in size, but maintains its shape. In the kinematic hardening material, the yield surface does not change in shape or size, but the centre of the yield surface moves. Mixed formulations of hardening are also available in many FE programs.

The relationship between strains and stresses beyond the onset of yielding is governed by means of *flow rules*. The flow rules define the direction of plastic strains beyond yielding. Most flow rules adopt *normality*, which implies that the plastic strain components vary such that their resultant is in the direction of normal to the yield surface.

In view of the rather complex nature of post-yield state of stress and strain, the solution is obtained by applying small increments of loading, and then summing up the displacement, strain and stress increments for each step.

2.4 Concrete

Crushing of concrete

The crushing of concrete is treated in much the same way as plastic yielding of steel. Some programs, such as ABAQUS, allow user defined stress-strain curves to be specified, which may allow computations for a falling branch of the concrete stress-strain characteristic.

Crack formation in concrete

For concrete, first of all separate material properties need to be defined for tension and compression. Because of its low tensile strength, concrete cracks, introducing discontinuities in the structure. There are two well-established methods adopted in FE analysis – the smeared crack approach and the discrete crack approach.

In the smeared crack approach, the cracks are assumed to occur at the Gauss integration points where the tensile stress exceeds the tensile strength. The extent of each crack is limited to the zone of influence of the integration point. Most FE programs permit tracking of the growth of tensile crack with increasing loads.

In the discrete crack approach, the crack zone geometry is redefined, and special gap elements are introduced which allow realistic modelling of crack behaviour, for example closure of cracks upon some reversal of local stresses.

It is recognised that the introduction of a crack reduces the stress across the crack to zero, but there still remains some capacity to resist tensile stresses in the vicinity of the crack. This is modelled through the device of tension softening, which assumes a gradual rather than abrupt reduction of tensile stress beyond the strain at which a crack first appears. This approach also offers superior numerical stability of the calculations.

Aggregate interlock

Because of the heterogeneous nature of concrete mixes, once a crack has been formed, there still remains a residual capacity to resist shear stresses along the direction of the crack. This is referred to as *aggregate interlock*. This effect can be modelled by specifying shear capacity as a function of the crack width.

Modelling of Reinforcement Bars

The simplest approach for modelling reinforcing bars is to design the mesh such that the reinforcement and the surrounding concrete share common nodes. The reinforcement bars can then be represented by pin-ended truss elements. This approach is effective when the reinforcement detail is, generally, parallel to the concrete boundaries.

An alternative approach is to use smeared reinforcement, sometimes also termed embedded reinforcement. In this approach the reinforcement bars do not necessarily conform to the mesh pattern of the surrounding concrete. The contribution to the element stiffness from the reinforcing bars is calculated by reference to the displacement of the concrete edges through which the reinforcing bars cross. It is necessary to assume either full bond between steel and concrete or zero bond.

Other effects in concrete

Most FE packages allow some other features of concrete to be modelled in the analysis. Most of these effects are such as not to influence the simulation of the behaviour of connections involving concrete. Such effects include, creep, shrinkage, crack dilation, and bond-slip between steel bars and surrounding concrete.

2.5 Timber

Modelling of timber poses yet further problems. Although predominantly elastic in nature, timber displays orthotropic properties – the material is strong along the grain both in tension and compression, but rather weak across the grain. The failure criterion commonly adopted is similar to plasticity in steel, but amended for the anisotropic behaviour. Good results have been reported by adopting Tsai's failure criterion [6]. For across the grain behaviour, numerical strategies similar to those for cracking in concrete can be used.

2.6 Contact and gap

Most commercial Finite Element programs offer some facility for dealing with the problem of contact and gap. Generally, the option is to use a node-to-node contact element or a node-to-surface contact system. While the node-to-node contact is simple to model, it is not always successful. For example, when simulating the contact between the bolt-hole and the bolt, the node to node arrangement underestimates the contact length. In some programs a few trials are often needed to determine the contact zone.

3 STUDIES BY THE NUMERICAL SIMULATION WORKING GROUP

The Numerical Simulation Working Group had, since its inception, a total of around 30 members from a similar number of institutions. At any given time, there have been around 10 active members. Apart from reporting on projects current in member institutions, the general approach agreed at the second meeting of the group was to select a number of types of connections and to ask members to conduct concerted studies. These were then reported and discussed at subsequent meetings. It was hoped that from these would emerge guidelines for analysts so that for any new type of connection the investigation process did

not have to start from the beginning. The intention was to focus on one each of a steel connection, a pre-cast concrete connection, and a timber connection. It was also felt that any conclusions drawn from the pre-cast concrete connection study would be relevant to steel concrete composite connections.

3.1 A Steel T-Stub Connection

A T-stub connection may be regarded as one of the simplest types of joints apart from a simple lap joint. In the context of the design of steel and composite connections by the "component method" as adopted in Eurocode 3 [1], T-stub becomes one of the principal components. A number of researchers have conducted experiments to build up the necessary load-deflection response of this component. The group decided that this should form the basis of its first concerted study. Test results were made available by Jaspart [7]. The schematic of the connection is shown in Fig. 1. The key points to emerge from these studies are given below. Many of the conclusions given below are derived from one or more of the working documents cited. Chapter 2 describes further studies in the modelling of steel connections.

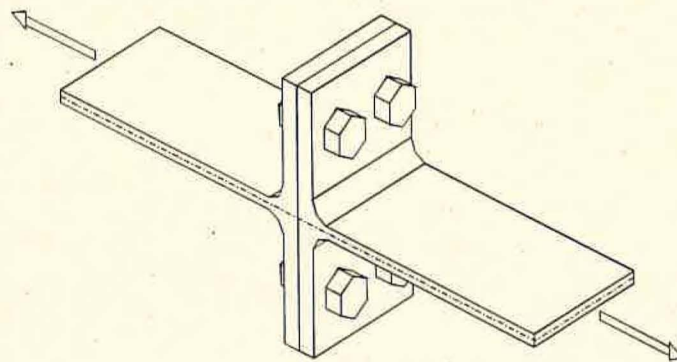


Figure 1 - The T-Stub Connection used for the first concerted study

Mesh

Where a plate component of a connection is likely to show flexibility, as in the flange elements of a T-stub, a certain minimum number of nodes through the flange thickness becomes necessary in order to simulate the eventual failure mechanisms in the element. It is generally agreed that 3 or 4 solid elements (8-node bricks) through thickness are necessary. In a similar manner, a circular hole, such as a bolt-hole would require a minimum of 12 to 16 nodes around the circumference (3 or 4 segments in each quarter).

Bolts

Simulation of bolts poses additional problems. Attempts, not very successful, have been made to model the bolt as a flexural element. In general, experience suggests that bolts need to be modelled using solid elements. Although they are small in size compared with the rest of the connection, they *are* the connection in most instances, and play a key role in the behaviour of the whole joint. In order to simulate the complex state of stress in the bolt, a reasonably refined mesh becomes essential. However, because this inevitably increases the

size of the problem, analysts are tempted to model the bolt as simply as possible. Also, because until the material yield spreads through the bolt, its behaviour is mostly elastic and may give the false indication that mesh refinement is not necessary. Thus, the differences in behaviour of the connection between a coarse mesh and a refined mesh for the bolt do not become apparent until the bolt demonstrates general yielding. Most successful simulations reported have adopted a fine mesh for the bolts.

There are additional aspects relating to the modelling of the bolt. Several of the studies in the past have, in the interest of expediency, ignored the role of the washer. The general conclusion would be to ignore the washer, unless it is modelled as a separate disk with sufficient elements through its thickness to model its flexure adequately.

Material Behaviour

For good correlation with experimental results, it is vital that full stress-strain characteristics of the constituent materials should be available. The data made available for the concerted study for T-stub connections [7] was found to be wanting in that the information on the stress-strain data for the bolt was not given, and only the grade was available. Recognising this gap, the team at Universität der Bundeswehr München has carried out careful experiments, which are described in Chapter 6.

3.2 A Pre-Cast Concrete Connection

The most common semi-rigid connections in concrete structures will be found in pre-cast concrete frames. The Numerical Simulation Working Group set up a concerted study for a pre-cast concrete connection (Fig. 2).

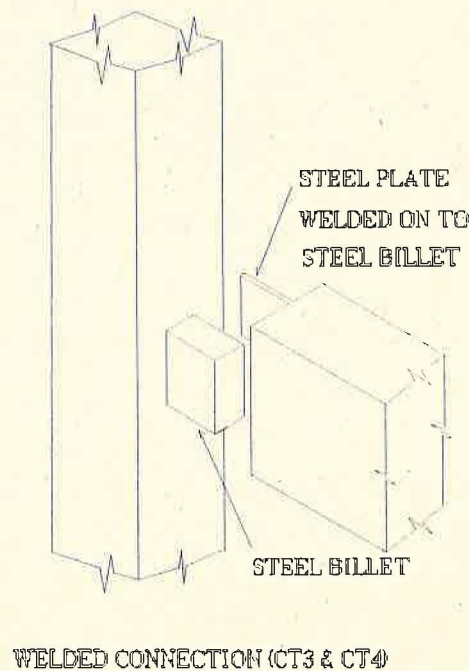


Figure 2 - The Steel Billet-Welded Plate Precast Concrete Frame Connection used for the concerted study

The data for the connection [8] was selected from a series of tests carried out at Nottingham University. The particular connection selected has a steel billet emerging horizontally from the column. A vertical steel plate cast in with the beam, and with appropriate anchor detail, is made to rest on the billet, and after locating the members correctly, the plate is welded to the billet. The space between the column and the end of the beam is then filled with *in situ* concrete. The resulting connection has been shown to give good moment capacity, marking it a suitable semi-rigid connection for competitive designs of pre-cast concrete frames.

3.3 Timber Connections

The range of timber connections includes dowel or bolted connections, gang nails, resin injected dowel connections, as well as joints with densified veneer wood coupled with expanded tube dowels. In view of the wide variation in the types of connections used in timber structures, it was not possible to set up a concerted study for timber connections.

Several comprehensive studies of the numerical simulation of timber joints have recently been carried out by Rodd [9], Schober [10], among others.

4 INTERPRETATION OF RESULTS FROM FINITE ELEMENT ANALYSES

4.1 Diagnostics

Most FE pre-processors offer warning messages on aspects of modelling. For example, such messages are often issued if the element aspect ratios are beyond a certain limit. Some diagnostic messages are issued if the input data is inconsistent. For example, if boundary restraints are specified for non-existent nodes, ignoring such messages may lead to not insignificant errors. In other cases, duplicate data may lead to doubling of nodal loads, resulting also in erroneous results. It is recommended that serious consideration be given to the warnings before deciding that they are inconsequential.

4.2 Stress Averaging

Care has to be exercised in interpreting the results from Finite Element programs. For instance, stresses may be output from a program at Gauss points, and this may form the basis of any contouring that the program may be able to show. When extrapolated to nodal points, this often leads to different stresses at the common nodal points of adjacent elements. Various algorithms are available in commercial programs to carry out the stress averaging at nodal points. Depending upon the procedure used, slightly different results may well be obtained.

4.3 Moment-Rotation data

The principal data obtained from tests on semi-rigid connections is the moment-rotation characteristics. In the context of design of connections, three aspects of this characteristic need to be quantified. These are the initial stiffness, the moment capacity and the ductility of the connection. In general, tests are conducted with a force being applied at some lever arm to generate a moment at the connection. From the geometry of the arrangement, it is

relatively easy to compute the value of this moment. However, what constitutes the rotation of the joint depends considerably on the instrumentation used. In a manner analogous to the experiments, numerical simulation by Finite Elements also requires a careful definition of what constitutes the rotation of the connection. Fig. 3 shows one possible approach that has been adopted by the team at City University. Clearly, if another definition is used, the rotations computed would be different, and this will affect any comparison with experimental results.

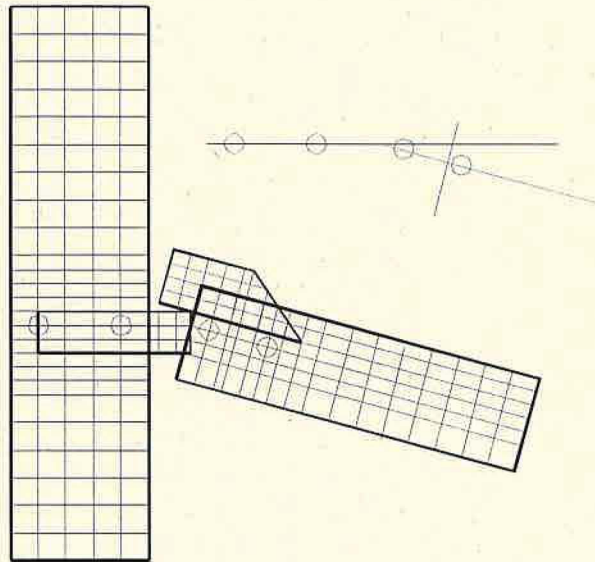


Figure 3 - One possible interpretation of joint rotation. In the connection zone, *in situ* Concrete has been removed for clarity

5. SOME RESULTS

As illustration of the progress made in the numerical simulation of connections, some results are presented here from some of the Working Documents to which reference has been made previously. Fig. 4 shows the correlation between experimental results for two mesh sizes made in 1995 by Viridi [11]. The results were obtained using the program ANSYS5.0. The mesh was made using 8 noded Solid45 elements. The fillet was represented by a single row of wedge elements. The stem of the bolt and the bolt head were modelled as one entity, with a gap of 1mm all round the bolt. Contact between the bolt and the plate was modelled using point to point contact friction element, Contact52. For friction Elastic Coulomb friction option was chosen. For the contact between the plates, a link element (Link 10) was used, with zero tension stiffness. Von Mises yield criterion was used for material yield. While the finer mesh gives good correlation with strength, and picks up the failure mode, it shows much higher initial stiffness than the experimental data. Many other researchers studying this particular experimental data have reached a similar conclusion.

More recent results for the same problem, obtained by Wald [12] using a later version of the same program, show considerable improvement. Much finer mesh all round, mainly in accordance with the recommendations made earlier for the plate, bolt, washer element, and

the fillet, has been used. Again, the option of point-to-point contact was adopted. However, instead of the 8 noded brick element, a 10-noded tetrahedral element was chosen. This offers better modelling for the bolt and the fillet. Broadly, good correlation with the initial stiffness range has been obtained, while the strength has been slightly underestimated, as shown in Fig. 5. Detailed results in the document also show how well the numerical simulation picks up the behaviour of the bolts.

NUMERICAL SIMULATION OF A T-STUB

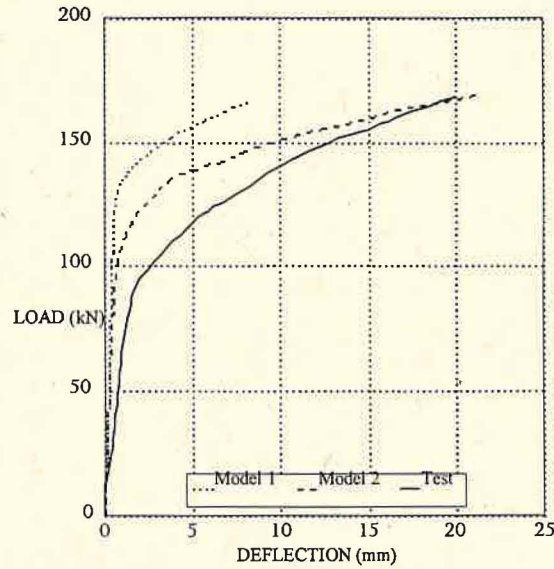


Figure 4 - Some early results from the T-Stub studies [11]. Models 1 and 2 refer to a coarse mesh and a finer mesh respectively.

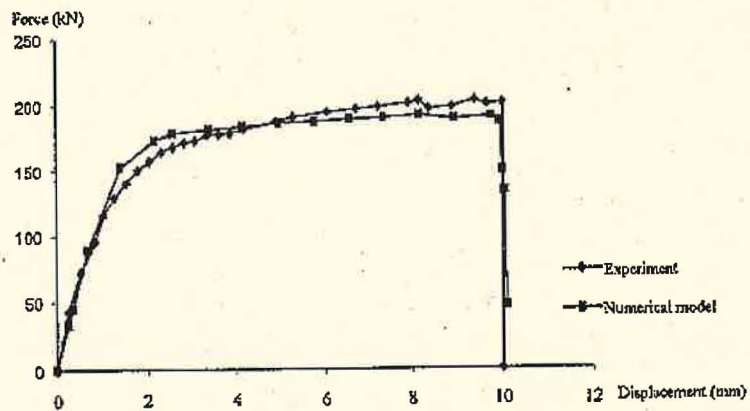


Figure 5 - Improved correlation between numerical and experimental results obtained in a recent study by Wald [12]

6. ORGANISATION OF THE REMAINING CHAPTERS

The activities of the Working Group have been presented through a selection of papers based on case studies at the three COST-C1 events [2]-[4]. It has been apparent for some time that universal "recipes" for performing numerical simulation using the Finite Element method do not really exist. Accordingly, the approach adopted in this publication is to illustrate the process of numerical simulation using the Finite Element Method through applications to a range of connections. Thus Chapter 2 deals with simulation of an end-plate connection and describes other complementary studies. Chapter 3 discusses the problem of simulating column base connections. Chapter 4 describes the relatively less studied problem of minor axis beam to column connections. The final Chapter describes a range of extensive tests conducted on simple connections to provide data for any future benchmarking computations.

7. CONCLUSION

The concerted work of the Numerical Simulation Group has led to some general guidelines to be adopted in performing a Finite Element based analysis of a given connection. One of the objectives has been to conduct further "numerical experiments", when successful simulation for a particular type of connections has been achieved. Members of the group have also benefited by learning from each other through reports on their own studies. In this context, unsuccessful applications have been just as useful as those in which good agreement with experimental results has been obtained.

REFERENCES

- [1] Eurocode 3. "Design of Steel Structures : Part 1.1 - General Rules for Buildings : Annex J on Steel Joints in Building Frames". *Paper No N419E CEN/TC250/SC3-PT9*. 1994.
- [2] *COST C1 Workshop - Control of the Semi-Rigid Behaviour of Civil Engineering Structural Connections*. Strasbourg. October 1992.
- [3] *COST C1 Workshop - Control of the Semi-Rigid Behaviour of Civil Engineering Structural Connections*. Prague. September 1994.
- [4] *COST C1 International Conference - Control of the Semi-Rigid Behaviour of Civil Engineering Structural Connections*. Liege, September 1998.
- [5] Johnson, W., and Mellor, P.B. *Engineering Plasticity*. Van Nostrand Reinhold Company, London. Pp70-72
- [6] Tsai, S.W., and Wu, E.W. "A general theory of strength for anisotropic materials". *Journal of Composite Materials*. Vol. 5, 1971, pp58-80.
- [7] Jaspert, J.P. "Numerical Simulation of a T-Stub - Experimental data)". *Working Document C1/WD6/94-09. Working Group 6 Meeting No 2, London, 1994*.
- [8] Elliott, K.S. "Precast Concrete Connection - Experimental Data". *Document C1/WD6/95-15. Working Group 6 Meeting No 4, Trento, 1995*.
- [9] Guan, Z W, and Rodd, P D. "A Simplified FE Model for Double Shear Joints made with a Hollow Dowel Fastener". *International Wood Engineering Conference, New Orleans, October 1996, pp 164-171*.

- [10] Schober, "Numerical Simulation of Timber Joints". *COST C1 International Conference Control of the Semi-Rigid Behaviour of Civil Engineering Structural Connections*. Liege, September 1998.
- [11] Ragupathy, P, and Viridi, K.S. "Numerical Simulation of a T-Stub Connection using ANSYS". *Working Document C1/WD6/95-16. Working Group 6 Meeting No 4, Trento, 1995.*
- [12] Wald, F, Villanova, F, and Zuhilke, A. "2-D and 3-D Modelling of a T-stub, the COST C1 example". *Working Document C1/WD6/97-03. Working Group 6 Meeting No 7, München, 1997.*

NUMERICAL ASPECTS FOR THE SIMULATION OF END PLATE CONNECTIONS

T. Wanzek & N. Gebbeken

University of the Federal Armed Forces Munich, Germany

In this paper the requirements will be listed which are necessary to perform reliable finite element analysis of end plate connections. For this purpose, the influences of the finite element model on t-stub connections will be checked by detailed numerical studies. In examples the numerical response will be compared with the Munich experiments in respect to the deformation, bolt force, and strains. At the end, the knowledge and the requirements will be transferred to general bolted end plate connections. In an example different moment initiation of a end plate connection will be discussed and their influence on the moment-rotation behaviour will be shown.

INTRODUCTION

Eurocode 3 allows the use of semi-rigid connections if their deformability is taken into account when predicting internal forces and deformations. The moment-rotation behaviour of the connections can be provided by an experimental based theory or directly by finite element analyses. Experimental investigations can be partially substituted by finite element simulations. This is advised for many reasons. Firstly, numerical simulations are not as time- and cost consuming as experiments. Secondly, numerical parametric studies are easy to conduct. In addition, they provide detailed information of the connection behaviour especially of the stress distribution and the plastic development in the material. On the other hand, up to now, the finite element analysis was not a reliable tool in order to forecast the load-carrying behaviour. The unreliability was based on two main reasons. First the unknown discretisation error with respect to mesh sensitivity, elements etc., and second, the lack of information about the experimental material data (entire σ - ϵ graph, static or dynamic values etc.).

Up to now, nearly all of the many experiments were performed to develop design criteria for "by hand" calculations of the overall behaviour (e.g. Zoetemeijer [5]) and not for the purpose of numerical simulations. As a consequence, a lot of experimental informations are missed, which are required for a detailed and exact numerical study. Therefore, Gebbeken, Wanzek and Petersen carried out t-stub experiments which satisfy such requirements. The detailed informations about the experiments are documented in the report [3] and an overview is given in the presentation "Benchmark Experiments for Numerical Simulation of T-Stubs" by Gebbeken and Wanzek in the present paper.

A fundamental numerical study which has been only partially performed before is as important as a detailed experimental study. But, a mesh convergence study

(discretisation error) and the precise investigation of the influences of different modelling is imperative in order to evaluate the reliability of the numerical results. It has to be clarified that the finite element method is an approximation method that may yield any big error. Here, the results of detailed numerical studies will be presented, which include also informations about influences of unknown experimental data (friction, imperfection). With the informations of these results at hand, the Munich t-stub experiments performed by Gebbeken, Wanzek and Petersen will be simulated by finite element analyses. Then, the knowledge will be transferred to general bolted end plate connections.

FINITE ELEMENT STUDIES OF T-STUBS

In the following finite element studies, two different t-stub models are used. The first t-stub model refers to the P1K experiment of the Munich series [3] and the second one is the Liege t-stub experiment. Usually, in this paper the Munich t-stub will be used because of its given detailed experimental data. But, especially the bolt influences will be checked at the Liege experiment as well, because the bolts were very stiff in comparison to the flange. Table 1 gives the informations, which are necessary for this study. The detailed characteristics will be given for the numerical simulations (see below).

The Numerical Model

The behaviour of t-stub connections is similar to the behaviour of the tension zone of bolted end plate connections. Therefore, the experiences obtained from the numerical t-stub studies can be transferred to general end plate connections. Keeping this in mind, the t-stub is generated with 3d finite elements.

Favourable for our finite element studies is the geometrical symmetry of t-stub connections. Therefore, only an eighth of the t-stub connection has to be modelled (Figure 1). The symmetry-plane between the two flanges is modelled by contact elements without friction at the rigid base (contact target in Figure 2). Certainly, because of the thread, the bolt elongation behaviour is not symmetric but the behaviour will be simulated as it is explained below. The nodes in the two remaining planes are fixed by symmetric geometrical boundary conditions (constraints vertical to the symmetry plane).

The material of each component of the t-stub model (rolled section, bolt, washer) is simulated by its individual material behaviour. For the following numerical studies it is assumed that flange and web material are identical, because the first failure mechanism is caused by plastic zones in the flange.

Numerical Bolt Model

In the numerical model the complicated bolt, composed of head, shank, thread and nut is simplified to a head and an "equivalent" shank. The equivalent shank is dimensioned in that way that it represents the half elongation behaviour of the real bolt (half because of symmetry). So the dimension of the shank represents the geometrical stiffness of the bolt. It can be stated that the influence of the bolt stiffness on the t-stub deformation as well as on the bolt forces significantly depends on the relative strength of the bolt. In the

Munich experiments, the bolts were very strong compared with the flange strength. Therefore, the bolt stiffness had nearly no influence on the t-stub behaviour. In contrast to the Munich experiments, the bolts of the Liège experiment were very weak compared to the flange. A bolt stiffness study (Figure 3) shows the little influence of the bolts. The curves 'Lbs1' refer to a bolt stiffness according to Agerskov [1] and the bolt stiffness of the model 'Lbs2' is only half of it.

The friction coefficient of both contact interfaces of the fastener bolt can vary between 0.1 and 0.5 (perhaps even bigger). Therefore, the influence of the friction coefficients is analysed in order to obtain possible deviations. An other aspect is the coupling of the bolt and the washer nodes. A coupled bolt-washer model is very useful, if flange imperfections are considered and the adjacent washer and flange surfaces are not parallel to each other. The numerical results show, that the numerical coupling of bolt and washer produces a stiffer deformation behaviour than the uncoupled model (Figure 4). But the difference between the high friction coefficient of model 'M-fc2' and the very small coefficient of model 'M-fc3' is negligible (friction coefficients in table 2). The bolt forces of the three models are nearly identical.

The magnitude of the prestressing force of the bolts primarily influences the initial stiffness (Figure 5). The limit loads do not vary significantly. This is as it should be from ultimate load theory.

Discretisation

The correct elementation and proper element types are, of course, main tasks in finite element modelling. The load-carrying behaviour of the flange or of the end plate, respectively, requires an element type that exhibits a good performance for bending dominated as well as plastic state problems. Because of the contact elements, the brick elements should not have midside nodes, i.e. 8-noded based brick elements will be applied here. In this work, the 8-noded 3d EAS-element (enhanced assumed strain) has been used. This finite element is based on a formulation of Simo, Amaro und Taylor [4]. It has been implemented in an inhouse fe-code. In several element studies, the EAS-element has shown excellent capabilities even in the plastic regime.

Flange Elementation

Main attention should be directed towards the elementation of the flange (respectively the end plate). This is because the deformation of this part usually dominates the behaviour of the whole connection. In addition it generates the most complex stress state with its bending in the plastic regime. Therefore, an element mesh as fine as possible with a discretisation defect as small as possible should be found while the calculations time should not exceed practical requirements. For this purpose, a discretisation study will be performed with respect to two parameters. The first parameter is the number of elements across the flange thickness in order to check capability of representing the development of plastic hinges accurately. The second parameter is the degree of discretisation in the flange (number of elements between web and hole and surroundings), in order to represent the strong bending problem of this part. The different elementations are labeled with 'Nx_{Fy}'. In the first part 'Nx', the number 'x' is identical to the number of elements across the flange thickness, and 'Fy' represents the degree of discretisation (Figure 6).

The deformation behaviour of the model with only one element across the thickness (N1F0) is obviously wrong (Figure 7). The model 'N2F0' is stiffer than the finer models 'N3F0' and N5F0' because the shear locking response overrules the plastic effects. If the discretisation between web and bolt becomes finer the typical response of bending dominated problems in plasticity is shown. The deformation behaviour of the models with more elements across the thickness are stiffer because the development of the plastic hinges (in the center still elastic) and zones is better represented (geometrical versus material stiffness). Therefore, for future studies the model with three elements across the flange thickness will be adopted. Next, a convergence study with respect to the elementation between web and bolt will be performed. The model 'N3F4' satisfies convergence requirements. The deviation from the model 'N3F3' is very small (Figure 8). Even the model 'N3F2' is applicable up to a gap of 3 mm.

Remark. From the "weaker" response of the models with less elements across the flange thickness, it should not be drawn the conclusion, that the weaker plastic response can compensate the shear locking effect. The global deformation behaviour seems to be identical but the stress distribution is quite different. The structural analysis has to satisfy the unique physical reality, locally as well as globally.

Bolt Elementation

The number of elements are determined decisively by the discretisation of the circumference of the bolt. For a bolt model with an area-equivalent square cross-section, only a few elements are needed. But the length of one side is less than the real diameter. In addition the quadratic form leads to a direction depending model and the sharp edges produce stress concentrations. Therefore, the square bolt model will not be considered here. The load-deformation curves and bolt forces of t-stub models with 8, 12 and 16 elements in bolt circumference are nearly identical. Consequently, the bolt model with 8 elements will be used. The influence of the remaining elementation will be determined by three different degrees of discretisation (Figure 9). Simulating both t-stub connections (Munich and Liege) the coarse bolt B0 overestimates the bolt forces. The bolt forces obtained by the models B1 and B2 are nearly identical.

Material Data

The required material data are prescribed by the used material model in the finite element analysis. For all numerical calculations, a rate- and temperature independent plasticity law with hardening is applied because the studies should be carried out for an ideal static situation. That means, the material data, provided by an experiment under a certain loading velocity, overestimates the static situation. Therefore, the loading velocity has to be set to zero from time to time in order to measure the real static response. This was the procedure at the Munich experiments. Therefore the static values, such as yield limit, has to be taken into account for the numerical material. Only in this case, a valid comparison between numerical simulation and experiment is possible.

The proportional relation (if flange failure occurs) between yield limit and ultimate load is generally known and will not be analysed here. But the influence of the consideration of the upper yield limit was numerically studied. For this purpose, the material function has been calibrated by the tensile test of the profile material. This

study revealed that there is practically no influence. This underlines the correctness of the former assumptions to neglect the upper yield limit.

Residual Stresses

The residual stresses of hot rolled sections mainly act in axial direction of the profile and can be of 50% of the yield limit. The remaining stresses in a little t-stub are very small, which can be simulated with finite elements. For the numerical calculations the residual stresses are produced by a thermal load distribution across the rolled section. The first example deals with the Munich t-stub and it is shown, that the residual stresses can be neglected (Figure). The second example is a t-stub without "free ends" that simulates a piece in the middle of a profile. Although the full residual stresses act in this model (e.g. like in a column) the difference between the model with and without residual stresses is small.

Imperfection of the Flange

It was measured in the Munich t-stub experiments, that the connected adjacent flanges were not parallel to each other. This was noticed by an initial gap under the web before the bolts were prestressed. From the gap measurement during the bolt prestressing. The magnitude of the initial gap was measured to be 0.5 – 0.6 mm. For a realistic comparison between the numerical model and experiments, the initial gap has to be considered because of its influence on the strain distribution as well as its influence on the development and distribution of plastic zones. The different approaches converge with respect to the strain curves when the limit state range is reached. The global deformation behaviour is nearly the same as obtained by the model without imperfection. But here it is intended to compare the strains of the numerical model with the experimental strains. Therefore, a quadratic imperfection function has been superimposed to the ideal geometry of the flange. The initial gap was set to be 0.3 mm (i.e. because of symmetry 0.6 mm in real).

SIMULATION OF THE T-STUB EXPERIMENTS

With the experience of the numerical t-stub studies the Munich t-stub experiments [3] have been simulated by finite element analyses. The numerical material can be formulated identical to the experiment's material, because the static stress-strain behaviour of the rolled section and the bolt characteristic (force-elongation) have been determined. With this at hand, it is possible to perform a realistic detailed comparison. Besides the gap (displacement) strains and bolt forces were compared as well. Thus a valid statement about the reliability of the finite element models will be possible.

Characteristics of the Numerical T-Stub Models

- Non-linear 3d 8-noded EAS-elements.
- Contact elements are generated between
 - washer and flange with a friction coefficient $\mu = 0.5$,
 - flange and symmetric rigid plane without friction.
- Washer is coupled with the bolt.

- Material of the section is calibrated with respect to the static stress-strain curve of the tension tests (Figure 10).
- The bolt material and the dimension size of the shank are calibrated with respect to the bolt elongation behaviour (Figure 11).
- Geometrical data according to the measured dimension (Table 3). Because of the hole clearance two simulations for each experiment will be carried out. Each simulation is generated with the extreme possible bolt position (see box in the corresponding diagram).
- Quadratic imperfection function to represent the non-parallel flanges with an initial gap of 0.3 mm (i.e. because of symmetry 0.6 mm in reality).
- Bolt forces after pretension:
 - $B_0 \approx 30$ kN at all PxK-experiments,
 - $B_0 \approx 100$ kN at all PxV-experiments.
- The load will be applied in a height of 160 mm at the web by constraints and these nodes are free during the prestressing of the bolt. The prestressing of the bolts is performed by constraints at the end of the bolt shank.

A detailed comparison between numerical simulation and experiment is performed at the Munich experiment P1K, for instance. The numerical results are compared with the experimental results in different ways. First the gap-load curve represents the global deformation behaviour. The gap is measured in a height of 40 mm at the web (Figure 1, $m_{\text{GAP}} = 80$ mm) and is set to be zero after the bolt is prestressed. Two numerical calculations with two extreme bolt positions (Table 3) have been carried out because of the slightly different hole positions and the hole clearance. The significant influence of the bolt position is shown in the deformation behaviour (Figure 13). The difference of the bolt forces of these two numerical simulations (Figure 14) is not so big in contrast to the strains at certain positions (Figure 12), which behave quite different (Figure 15) depending on the bolt position. Nevertheless, the qualitative and quantitative response of the numerical simulations with respect to the deformation, forces, and strain correspond to that of the experiments. The numerical simulations of the other Munich experiments show the same correspondence with the experiments, e.g. the experiment P2K (Figure 16). The good correspondence with the experiment of Liège (Figure 3) is not a valid statement for the reliability of the numerical models used, because in this case only the global deformation behaviour can be compared with the experiment. Unfortunately, some experimental information are missed.

REQUIREMENTS FOR A RELIABLE SIMULATION

The experiences of the numerical t-stub studies will now be summarized in a list of requirements which are needed for reliable simulations. These requirements can be transferred to general bolted end plate connections. The statements about the discretisation are only valid for element types similar to the here used EAS-element.

- Flange discretisation between bolt and web:
 - Elementation depends on bending in this part.
 - Mesh convergence study is necessary.
- Discretisation in thickness direction:

- Two or three elements are minimum
(depending on relative thickness, element type and integration points).
- Contact:
 - Penetration controlling contact algorithm (e.g. Augmented Lagrangian)
 - Coupling of washer and bolt is possible but leads to a little stiffer deformation behaviour.
- Material data:
 - Static material data for static analysis.
 - Real hardening data should be used.
 - Upper yield limit can be neglected.
- Possible imperfection has to be checked:
 - Bolt position and possible hole clearance
(significant influence on the t-stub).
 - Initial gap (important for detailed studies).
- Residual stresses:
 - Neglectable in short pieces because the remaining stresses are small.
 - Even under full residual stresses the influence is small
(e.g. column at a beam to column connection).
- Bolt:
 - The connection's sensitivity with respect to the bolt stiffness should be estimated by calculations with two extreme possible bolt characteristics.

By complying with these requirements a reliable numerical investigation of end plate connections with the finite element method is guaranteed. Only the initial stiffness of the numerical simulations were weaker. But, usually only the very first part differs from the experimental stiffness as it is shown in the gap-load behaviour of the Munich experiments P1K and P2K (Figure 13 and 16).

SIMULATION OF END PLATE CONNECTIONS

With the knowledge about the influences on t-stubs, end plate connections can be modelled. The requirements of the t-stub connections can be transferred to the analogous parts of the end plate connection, i.e. to the bolt region in the tension zone. In addition to these requirements the attention is focused on the consideration of the bending moment which is the load. There are two different ways to generate the moment at the end plate connection (Figure 17). First, a stress distribution which can be applied at the beam, and secondly, a shear force can be used. In the first case (case 1) the pure moment is considered, which has the big advantage, that the contact between bolt shank and end plate or any constraints along the plate do not have to be considered. But, the distance between the stress initiation and the end plate has to be large enough, because the distribution in the beam profile near the end plate is quite different to what is usually assumed in the middle of a beam. In the other case (case 2), applying a shear load at the beam, the bolt shank contact has to be modelled. This needs special attention with respect to the contact condition between bolt shank and inner hole surface. Certainly, the consideration of the shear force leads to the more realistic modelling of the connection.

But, it will be shown in an example, that the deviation in the moment-rotation behaviour of the connection between case 1 and case 2 does not occur if the shear stress is small in relation to the normal stress. For this example we choose one of the end plate connection experiments from Bernuzzi, Zandonini and Zanon [2] (Figure 17). The deformation and the plastic zones of the finite element calculation are shown for an applied moment of 100 kNm (Figure 20). The moment of the numerical calculation 'ep-m' is applied by a moment stress distribution at the end of the beam, i.e. in a distance of 300 mm from the rigid base. In the second calculation 'ep-p' a shear force is applied at 1000 mm similar to the experiment. The moment-rotation behaviour is shown (Figure 18) in relation to two different rotation definitions (Figure 19), the connection rotation Φ_{cn} and the total rotation Φ_{tot} . The total rotation, which was measured in a distance of 300 mm, relates to the kind of loading (Figure 18), because the stress state in the beam is different. On the other hand, the connection rotation Φ_{CN} as a sum of the bolt elongation and the end plate deformation is identical in both loading cases. This fact underlines that the connection rotation is the unique measurement analogous to the gap in the t-stubs.

REFERENCES

- [1] Agerskov, H.: High-Strength Bolted Connections Subject to Prying. Journal of Structural Division, ASCE, 102 (1976), 161-175
- [2] Bernuzzi, C., Zandonini, R., Zanon, P.: Rotational Behaviour of End Plate Connections. *Costruzioni Metalliche*, 2 (1991), 74-103
- [3] Gebbeken, N., Wanzek, T., Petersen, C.: Semi-Rigid Connections, T-Stub Modelle – Versuchsbericht –, Report on Experimental Investigations. *Berichte aus dem Konstruktiven Ingenieurbau der Universität der Bundeswehr München*, Nr. 97/2, ISSN 1431-1522 (1997)
- [4] Simo, J.C., Amaro, F., Taylor, R.L.: Improved versions of assumed enhanced strain tri-linear elements for 3D finite deformation problems. *Comp. Methods in Appl. Mech. and Engrg.*, 110 (1993) 359-386
- [5] Zoetemeijer, P.: A Design Method for the Tension Side of Statically Loaded Bolted Beam-to-Column Connection. *Heron*, Vol. 20, Technische Hogeschool Delft, 1974

Tables and Figures

- Table 1: Geometry of the Munich P1K and the Liege experiment.
- Table 2: Friction coefficients of the contact study.
- Table 3: Dimension size of the performed simulations.
- Figure 1: T-stub connection with characteristic measurements and denotation. Marked area shows the part which is numerically modeled.
- Figure 2: A Finite element model with symmetry boundaries.
- Figure 3: Study with two different bolt stiffnesses. Liege experiment.
- Figure 4: Study with different friction coefficients (Table 2). Munich experiment.
- Figure 5: Influence of the bolt pretension. Munich experiment.
- Figure 6: Discretisation study. Elementations of the N3Fy-series.
- Figure 7: Discretisation study. Number of Elements across flange thickness. Munich experiment.
- Figure 8: Discretisation convergence shown by the N3Fy-elementations. Munich experiment.
- Figure 9: Bolt Discretisation. Three bolt elementation each with 8 elements around the circumferences.
- Figure 10: Comparison between the material of the experiment and of the numerical models by the tensile test. Munich experiments.
- Figure 11: Elongation behaviour of the bolts. Munich experiments.
- Figure 12: Location of the strain gages. Munich experiments.
- Figure 13: Global deformation behaviour. Gap-load curve of the Munich experiment P1K.
- Figure 14: Bolt force behaviour. Munich experiment P1K.
- Figure 15: Strain behaviour (positions in Figure 12). Munich experiment P1K.
- Figure 16: Global deformation behaviour. Gap-load curve of the Munich experiment P2K.
- Figure 17: Experiment EP1-1 from Bernuzzi, Zandonini and Zanon [2].
- Figure 18: Finite element analysis. Moment-rotation behaviour of the experiment EP1-1.
- Figure 19: Definition of different rotation.
- Figure 20: Deformation and plastic zones. Finite element analysis of the experiment EP1-1.

| | Profile | Bolts | dimension size in mm | | | |
|------------|---------|-----------|----------------------|-----|-------|-----------|
| | | | e_2 | l | p_2 | m_{GAP} |
| Munich P1K | IPE 300 | M16, 10.9 | 25 | 105 | 25 | 80 |
| Liege | IPE 300 | M12, 8.8 | 30 | 80 | 20 | 300 |

Table 1:

| | Numerical models | | |
|----------------------|------------------|---------|---------|
| | Mfc1 | Mfc2 | Mfc3 |
| friction coefficient | | | |
| bolt - washer | 0.50 | coupled | coupled |
| washer - flange | 0.30 | 0.50 | 0.01 |

Table 2:

| | edge distance [mm] | | | IPE 300 [mm] | | | | |
|---------|--------------------|---------------|-------|--------------|-----|-----|------|------------|
| | $e_{2, hole}$ | $e_{2, bolt}$ | p_2 | l | b | s | t | h_{load} |
| Munich | | | | 210 | 151 | 7.1 | 10.4 | 160 |
| P1K bp1 | 24.8 | 23.8 | 25.0 | | | | | |
| P1K bp2 | 24.8 | 25.8 | 25.0 | | | | | |
| P2K bp1 | 25.0 | 24.0 | 60.0 | | | | | |
| P2K bp2 | 25.9 | 26.9 | 60.0 | | | | | |
| Liège | 25.0 | 25.0 | 20.0 | 80 | 150 | 7.1 | 10.7 | 150 |

Table 3:

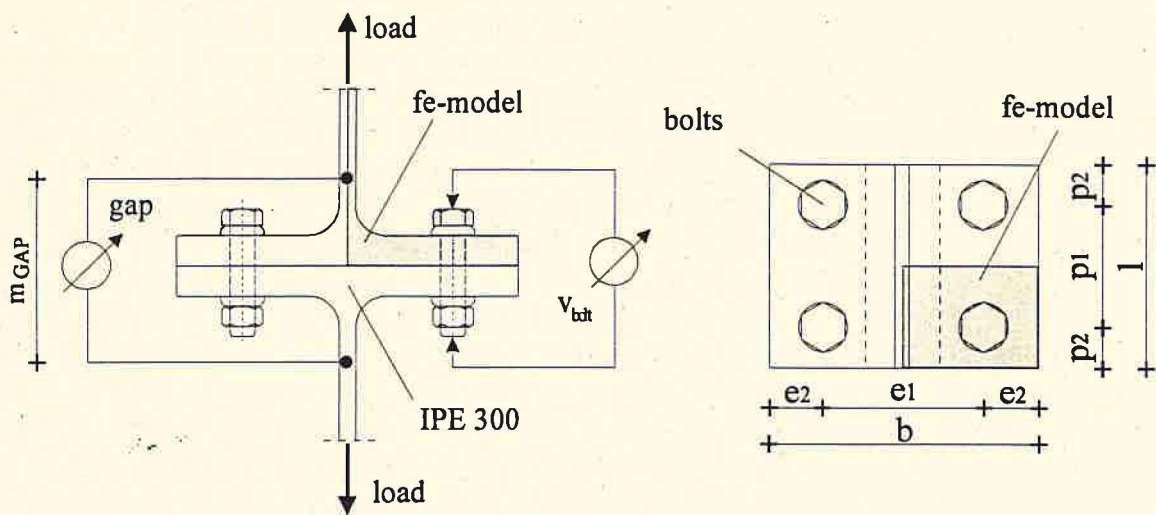


Fig. 1:

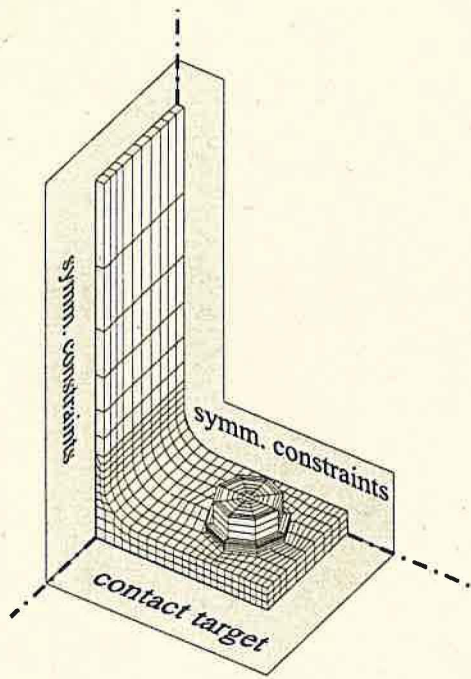


Fig. 2:

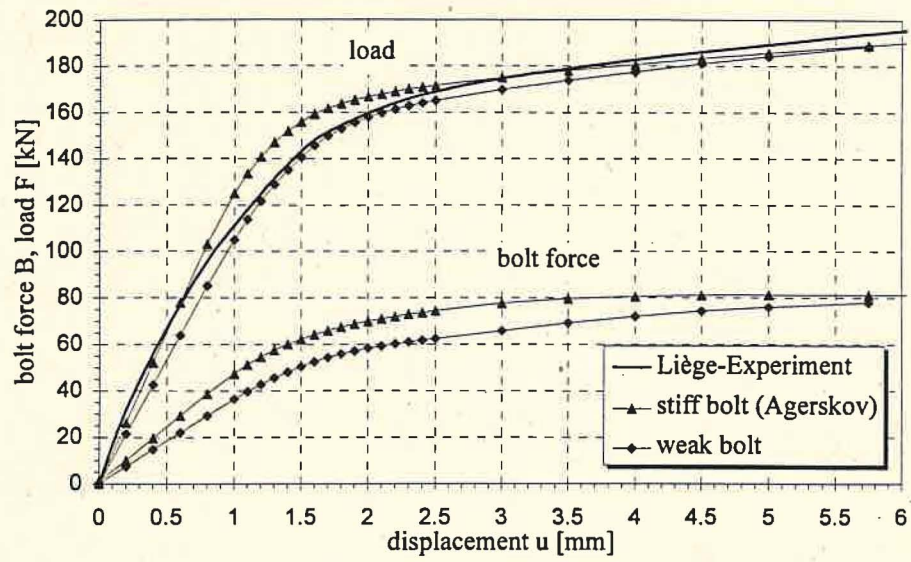


Fig. 3:

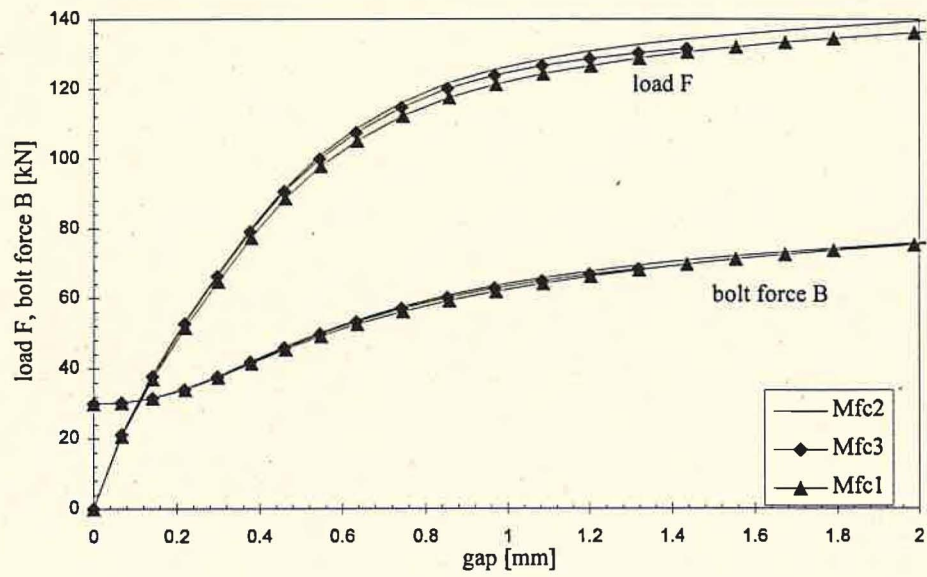


Fig. 4:

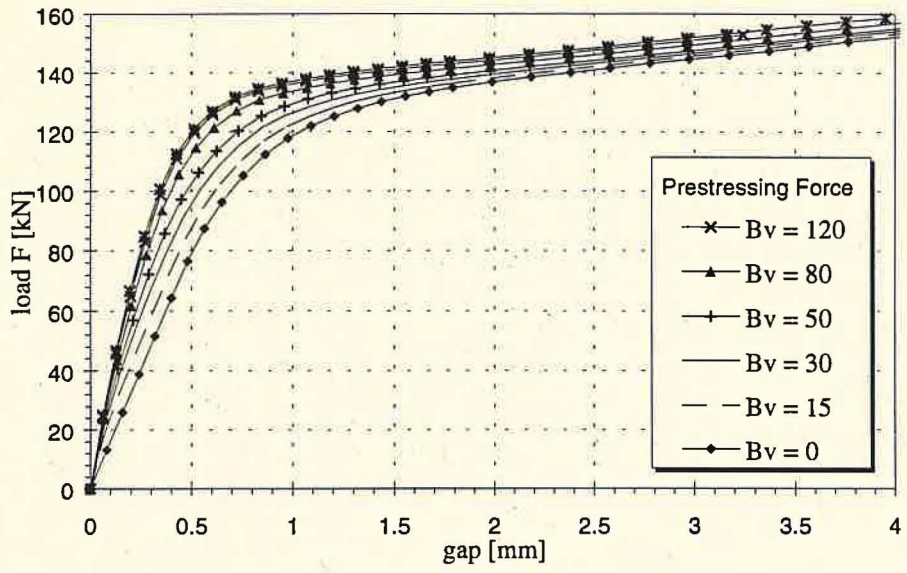


Fig. 5:

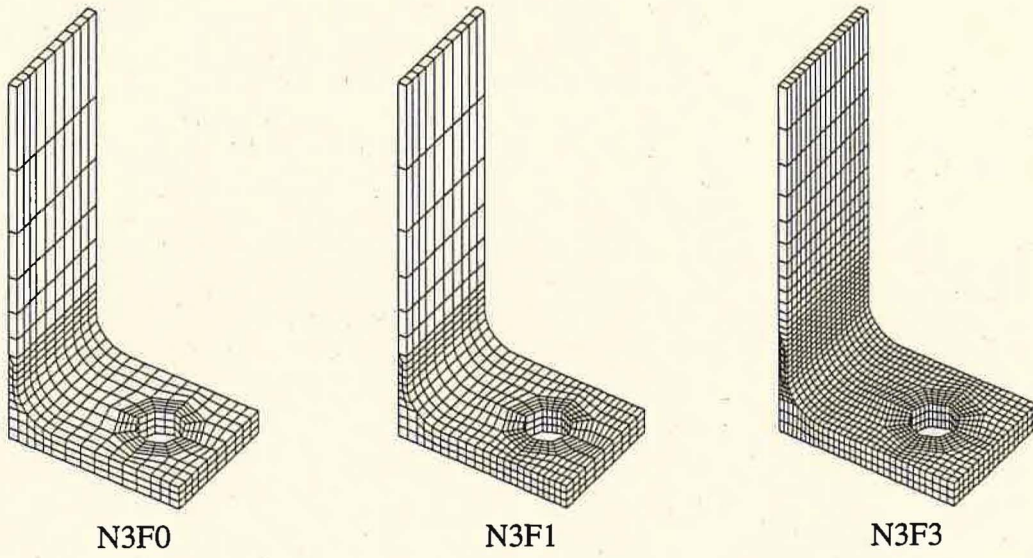


Fig. 6:

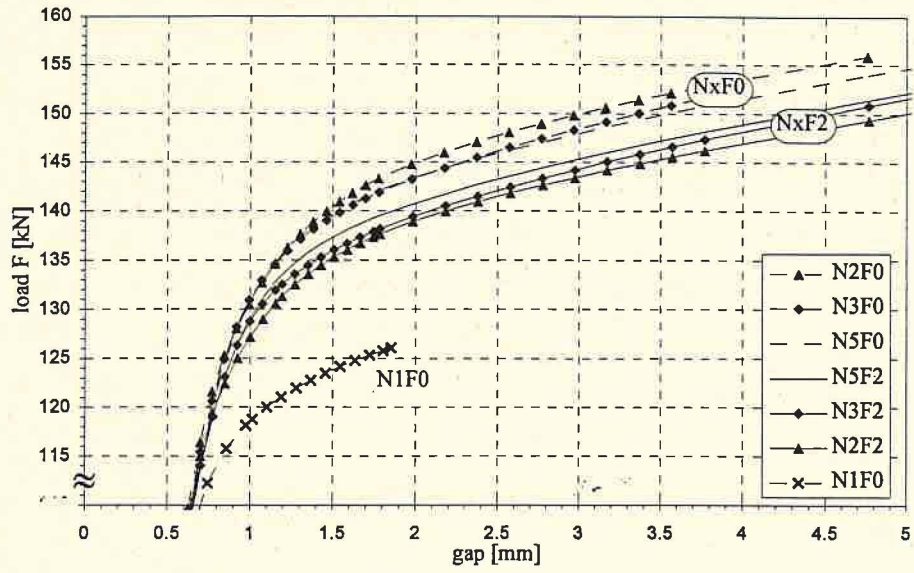


Fig. 7:

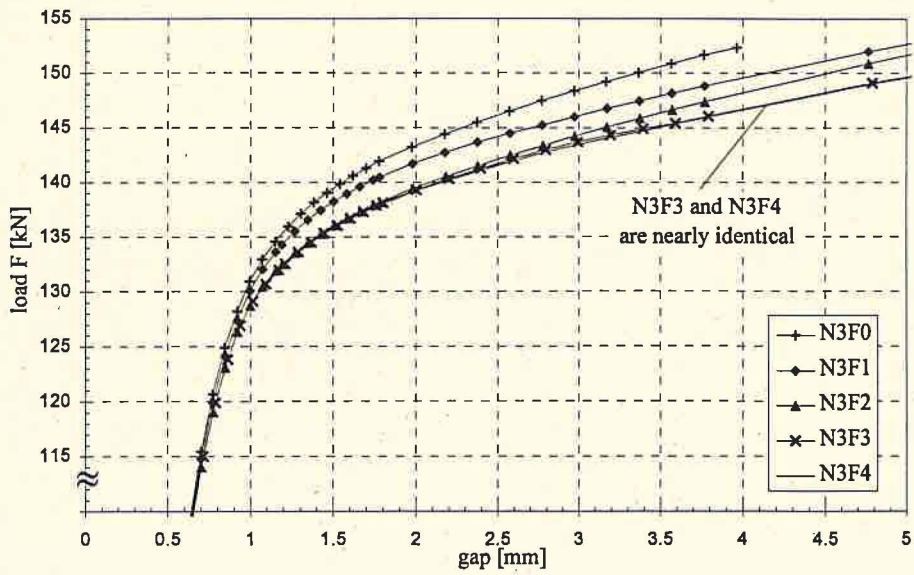


Fig. 8:

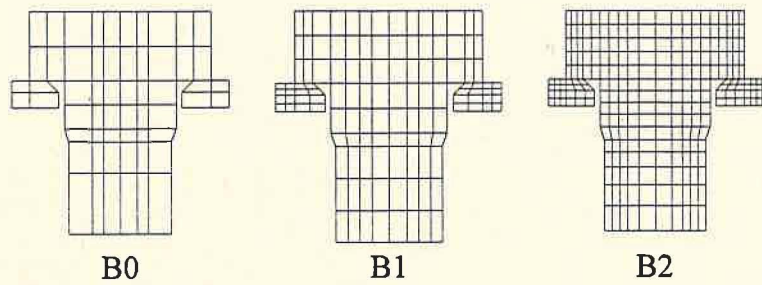


Fig. 9:

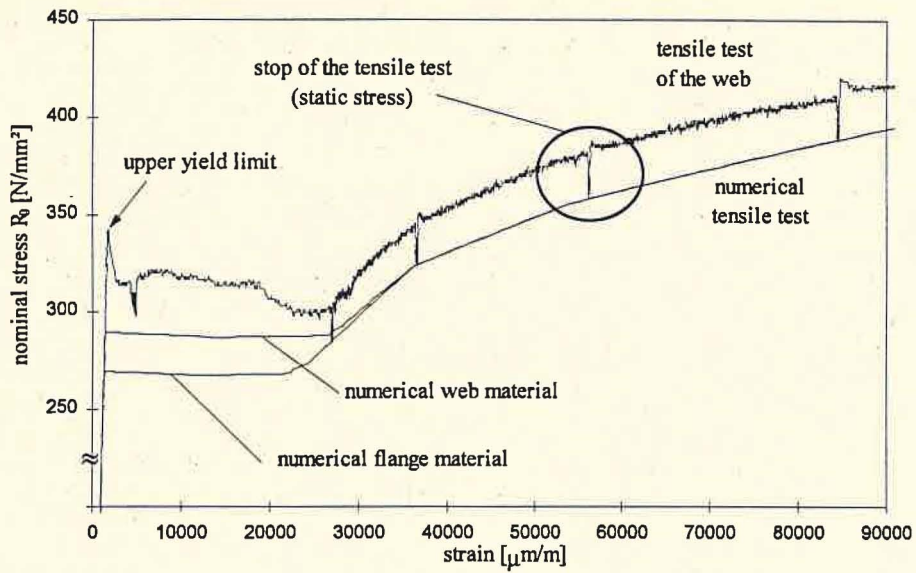


Fig. 10:

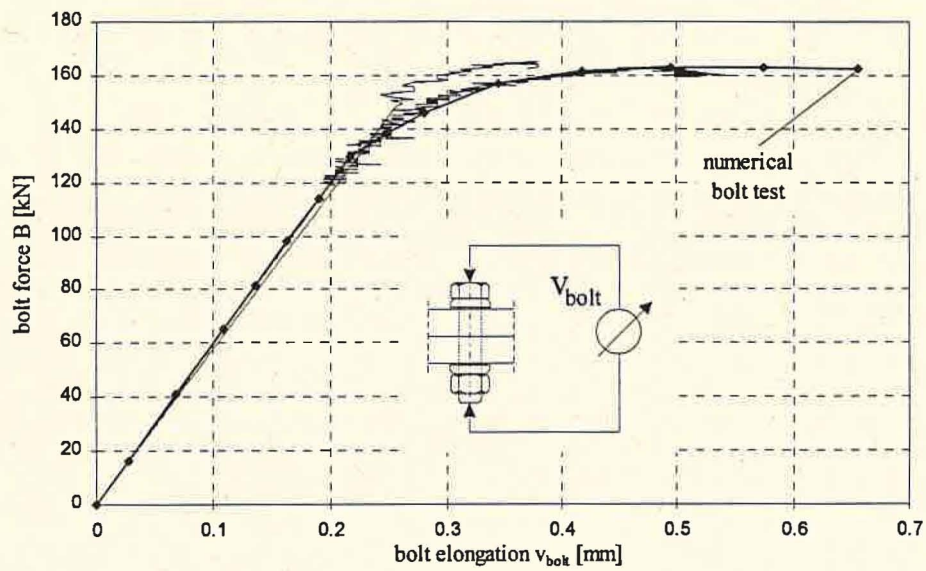


Fig. 11:

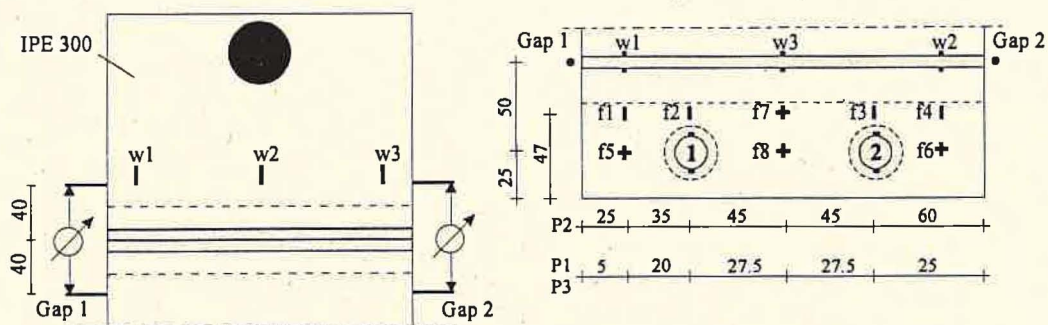


Fig. 12:

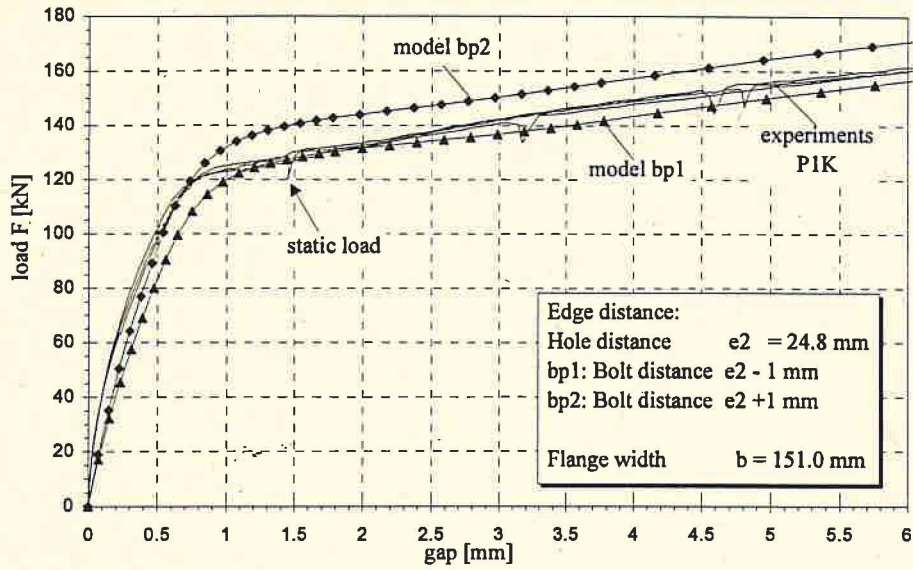


Fig. 13:

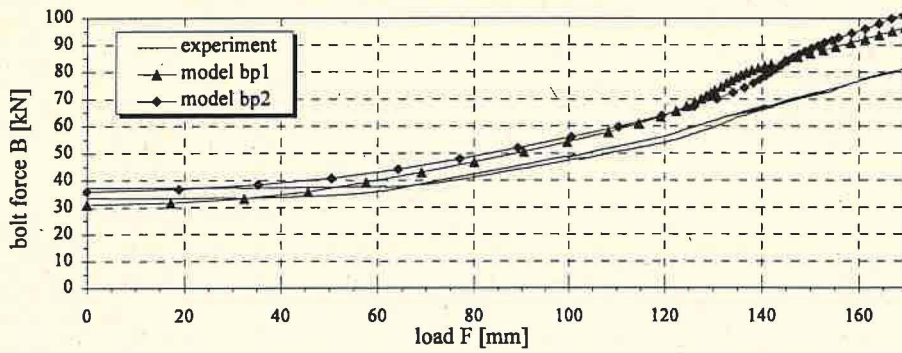


Fig. 14:

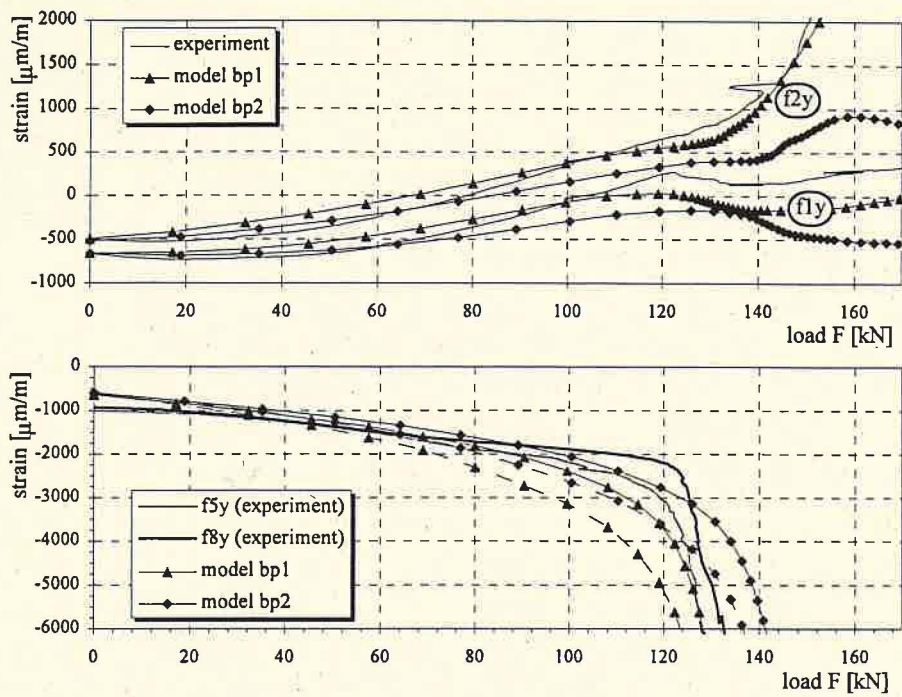


Fig. 15:

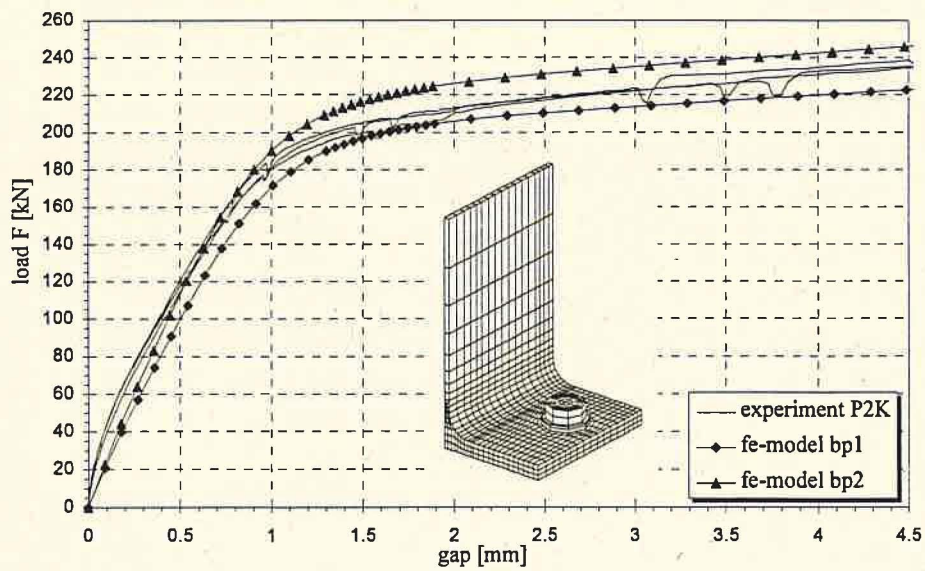


Fig. 16:

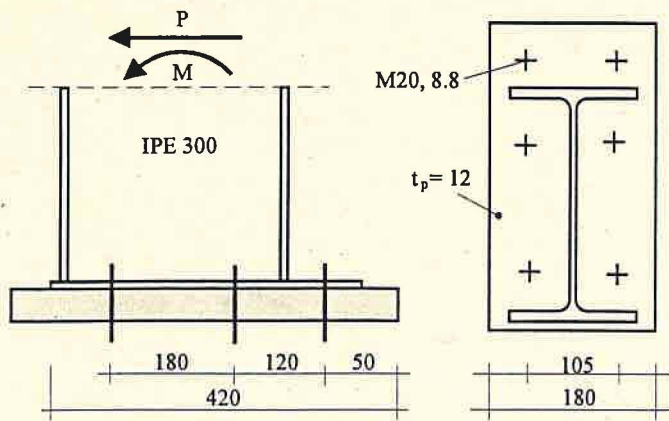


Fig. 17:

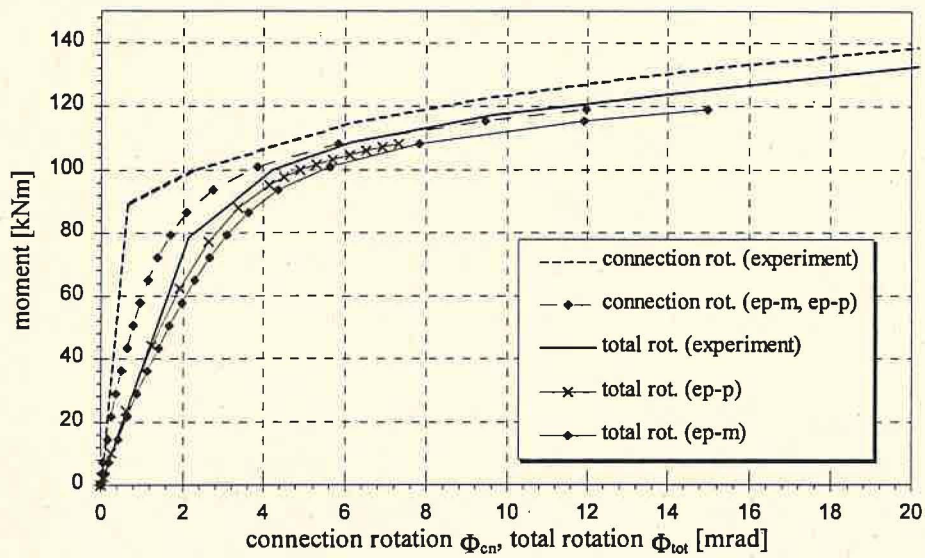


Fig. 18:

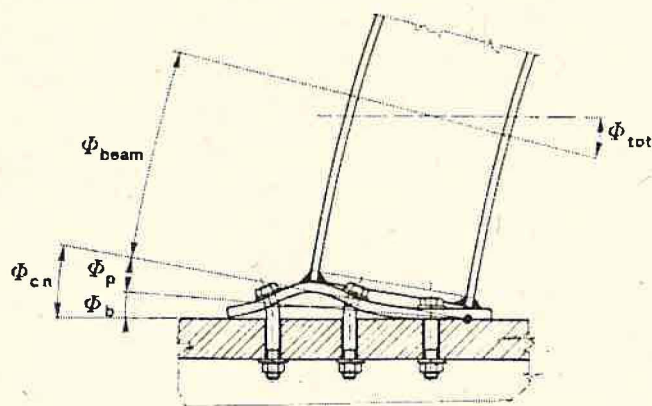


Fig. 19:

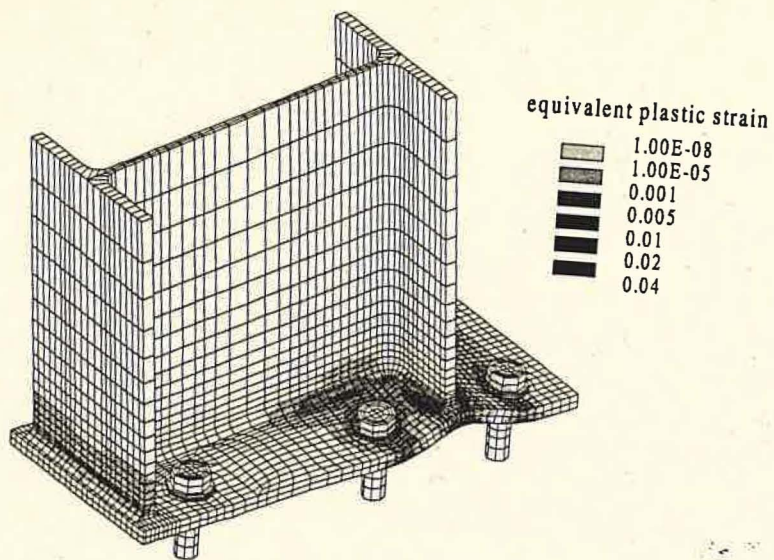


Fig. 20:

COLUMN BASE CONNECTIONS

Ch. C. Baniotopoulos
Aristotle University of Thessaloniki, 540 06 Thessaloniki, Greece

Z. Sokol, F. Wald
Czech Technical University, 166 29 Praha, Czech Republic

ABSTRACT: The paper presents comprehensive information about numerical modelling of column bases of steel structures. It deals with particular aspects of the modelling and describes their importance and influence on the overall behaviour of the model. It also introduces an effective 2-D numerical model and in addition, two experiments of two basic components of the column base connection which may be used as calibration examples of the calculation. Examples of numerical computation are presented.

1 INTRODUCTION

The present paper aims to contribute to the research efforts concerning the numerical modelling of column base connections. In particular, it deals with certain aspects of the modelling and describes their influence on the overall behaviour of the model. As known, the stress states of a column base connection under static loading has to be computed by appropriate models that are capable to take into account two critical parameters: the development of plastification zones, local crushing and cracking of concrete block, transfer of shear force under the base plate, the different anchoring influence and the unilateral (frictional or not) contact effects on the interfaces between connection members.

Through recent years, numerical simulations of steel connections have been described by one-dimensional to three-dimensional models. The one-dimensional (Bernoulli beam) models of such connections (bolts modelled as springs), taking into account only primary bending action, are naturally the most simple. On the other hand, a three-dimensional model can incorporate all the essential features of the steel connections, leading in general to the most accurate results. This is due to the fact that three-dimensional models, having been appropriately formulated and computed contain the correct stress distribution patterns, but in a form that requires great computational effort. The first attempts for two- and three- dimensional modelling of steel connections based on several simplified assumptions, are dated back to the seventies; these efforts are till nowadays continued by deducting one by one the simplifying hypotheses of the initially proposed models, thus producing more and more interesting and realistic results [5, 9, 14, 24]. In the present paper, we first present a two-dimensional finite element plane stress model which has been constructed for the analysis of the structural behaviour of a column base plate connection [13]. The model contains all the essential features that characterise the

separation problem. Material yielding, contact interface slip and interface interaction are taken into account. Secondary bending effects are not present due to the static loading. The third dimension of the connection, is also considered by assigning different thickness values to the various regions of the FEM. mesh, thus achieving the most realistic response of the two-dimensional model.

The applied numerical method, does not use any a priori assumption on the flexibility of the several parts of the steel connection, to obtain first its deformed shape where contact (i.e. compressive reaction) and separation (i.e. tensile reaction) zones have been developed and next the actual stress distribution on the connection members by taking into account friction effects on the interfaces. The proposed finite element model is constructed in a way, that the interaction at any interface of the connection can be taken into account by means of unilateral contact boundary conditions [4-8, 13, 20]. Following this method, local separation zones between the interfaces of the steel connection are computed, whereas the deformed shape of the steel connection is with accuracy evaluated. Note also that the numerical results calculated by applying the proposed two-dimensional model, qualitatively conform well to those obtained by pilot experiments [12, 18]. Within such a theoretical framework the separation, the active contact, as well as the plastification zones are with accuracy calculated, leading thus to the computation of the exact stress state conditions holding on the steel connection under investigation.

2 FE MODELLING

The proposed numerical method, seems to be a reliable tool for the numerical simulation of the structural behaviour of most types of steel connections, because from one side the response of the different parts (column, plate, bolts) of the modelled steel connections are taken into account in an interactive way, whereas on the other side, the correct thickness of the various parts of the two-dimensional model are defined by applying an efficient and easy technique [19].

The numerical treatment of such problems also permits the investigation of the appearance of prying action forces. In the case of the column-base plate connection, the prying action phenomenon is directly connected with the flexibility of the connections. Exactly opposite is the reaction in the case of steel column-base plates, with underlying concrete foundation. The difference is due to the fact, that the one part of the connection (concrete foundation) is not deformable and this leads this way the deformable base plate to be locally separated from the concrete surface. As is obvious, the thickness of the base plate, is one of the most significant parameters that affects the response of such steel connections. Therefore, considering the thickness as a critical parameter for the analysis of the connection interface, under various axial external forces and moment rotation, such a sensitivity analysis should be considered as a contribution to the research of steel column base plate connections. The sensitivity study of a numerical application takes into account the base plate thickness as the critical parameter of the analysis. The obtained results are of great interest showing the different response of each connection of different base plate thickness under different loading conditions.

Applying an appropriate finite element model, the stress flow between the various components of a column base connection has to be followed up, whereas the main deformation and stress distribution patterns must be present and directly recognisable and interpretable. An

appropriately defined 2-D plane stress model encompasses all the thickness effects, primary bending/membrane effects and the contact stress distribution on the connection interfaces between the parts of the connection. Stress concentration zones can be easily identified although the analysis remains incomplete, whereas secondary bending effects are not present in the model, but they cannot drastically affect the whole picture of the stress fields due to the static external loading. Such a 2-D model takes into consideration the dimensions of the joint also along the third direction by assigning different thickness values to the various regions of the FEM mesh, thus achieving a realistic simulation of the overall response of the model. In the regions where the thickness cannot be directly prescribed, as is e.g. the neighbourhood of the bolts, the washers and the zones with holes, several different assumptions have been made and the respective results have been compared to accurate numerical models which take into account the exact thickness value of each finite element. Although the later model gives the most accurate numerical results, the task of assigning the thickness of each region is a rather time consuming work. Thus, comparison of the results of the various tries of 2-D modelling is in any case unavoidable, in order to estimate the errors introduced by rougher assignments of the thickness of each part which requires less effort. To conclude with, we note that the applied 2-D model offers the following advantages: (i) Accurate numerical results in the cases that the geometry of the connection and the loading conditions, lead to 2-D deformed configuration, (ii) minimum computational costs and evaluation save of effort and (iii) they can be applied for reliable quick benchmark tests in validating commercial 3-D finite element codes for the analysis of steel connections.

3 COST-C1 BENCHMARKS

The experiments prepared for COST C1 calibration example represent both basic components of column base joint and anchor bolt. They were chosen from a wider set of experiments carried out at Czech Technical University in Prague, see [23].

Knowledge of material properties is important for numerical modelling therefore great care was taken to material tests, for details see [23]. The concrete used for the blocks was designed as C35. Compressive strength and modulus of elasticity were measured. The compressive strength $f_{cd} = 33,1 \text{ MPa}$ and modulus of elasticity $E_c = 46\,789 \text{ MPa}$. The modulus of elasticity was measured by ultrasonic method. Material properties of the steel were obtained from tensile tests. The yield stress $f_y = 334 \text{ MPa}$ and ultimate strength $f_u = 460 \text{ MPa}$ were found for T-stub in compression, $f_y = 317 \text{ MPa}$ and $f_u = 400 \text{ MPa}$ for T-stub in tension and $f_y = 365 \text{ MPa}$ and $f_u = 443 \text{ MPa}$ for the anchor bolts.

The basic component influencing the tension part of column base is the anchor bolt. For COST C1 numerical simulation was chosen the example of typical steel frame anchoring, the anchor bolt with anchor head, see Fig. 1. The deflection was measured 25 mm from the concrete surface, see Fig. . Two pull-out test of single anchor bolt were performed to find out strength and stiffness of the bolt. The load-deflection curve exhibits bi-linear relationship with stiffness $334,1 \text{ kN/mm}$ and ultimate strength $199,2 \text{ kN}$. The bolts failed by damaging of the threads. The load to T-stub was applied in equal steps. Five loading/unloading cycles were performed prior loading up to collapse. At each load level, vertical displacement of two points on centre line of the base plate were measured. The load-displacement diagram is shown on Fig. 1. Separation of the base plate from the concrete was clearly observed during the loading

cycles. Plastic hinges in the base plate developed later which led to increasing of deformation. At load 272 kN both bolts broke.

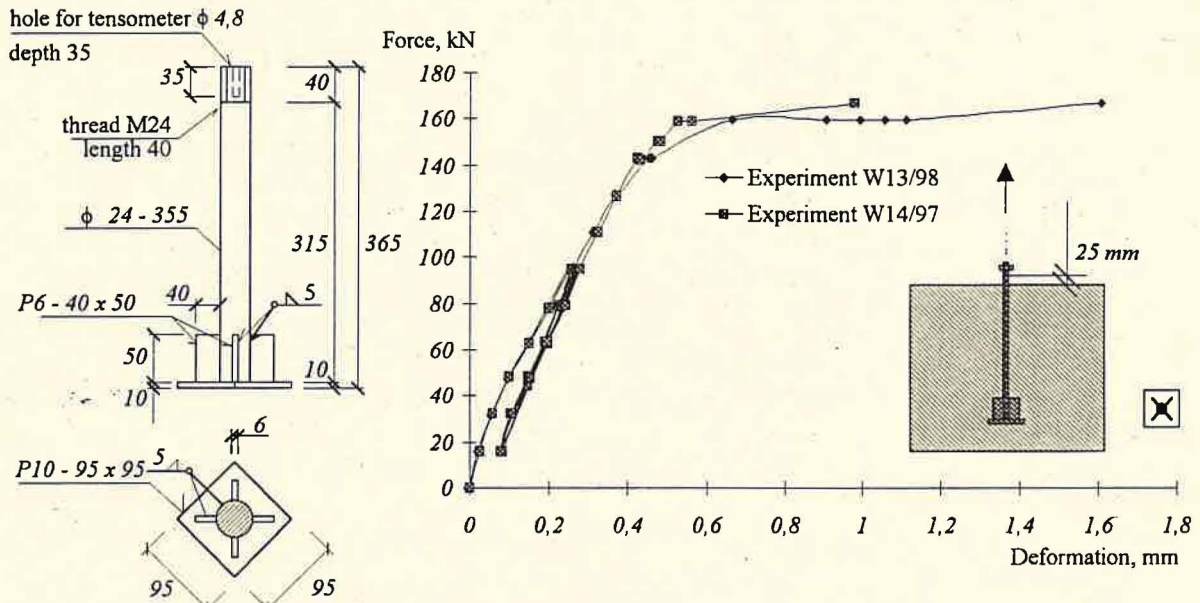


Fig. 1 The deformation of the anchor bolt, geometry of the anchor bolt [23]

This experiment for calibration example for the component in tension was chosen from twelve similar tests. It is referred as W97-03 in a comprehensive research report, see [23]. The experiment with T-stub in tension was especially focused on observing deformation of the T-stub loaded by tensile forces, evaluating the bolt force and prying effect of the anchor bolts, observing different failure modes of the T-stub (plate yielding, plate yielding and bolt failure, bolt failure), evaluating the ultimate load of the T-stub. The test specimen, see Fig. 2, was attached to concrete block of size 550 x 550 x 550 mm. No grout was used at the contact area but only thin layer of plaster was used to achieve smooth and level contact surface. The anchor bolts used for fastening of the T-stub are shown on Fig.. Each bolt was equipped with a tensometer placed in a hole in the bolt shank. Hand tightening of nuts and one washer was used for this test.

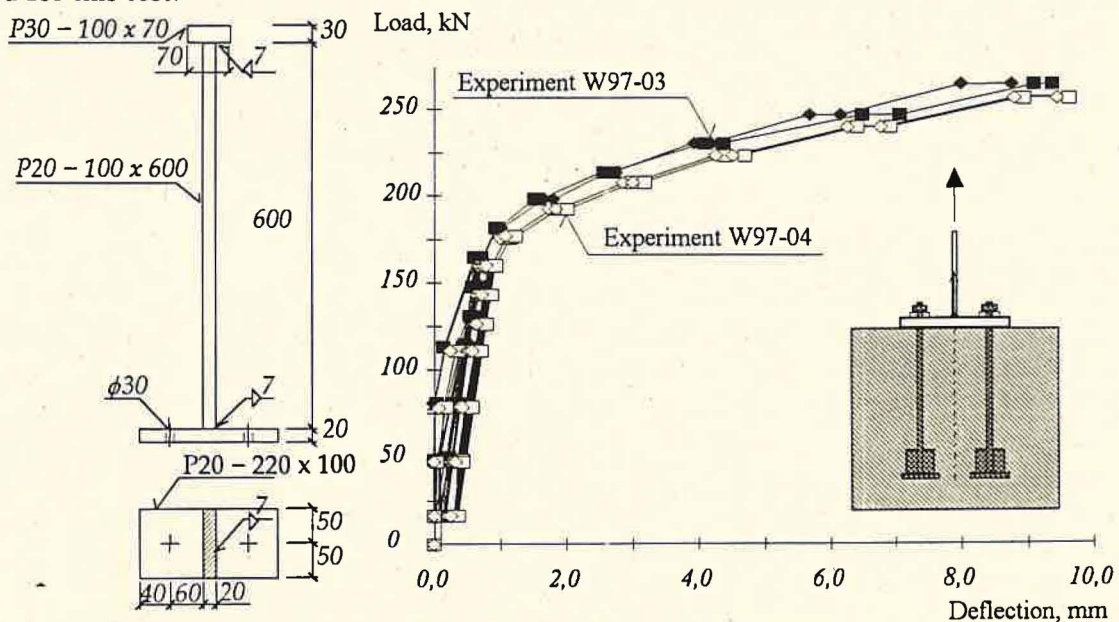


Fig. 2 Load-displacement curves of test in tension, geometry of the test [23]

The test simulates base plate loaded by the compressive force from the column flange. The test specimen consists from a steel plate and a rectangular steel bar representing the column flange. The bar is not welded to the plate but simply laid across, see Fig. . Thin layer of plaster was used instead of the grout to ensure proper contact of the plate and the concrete. Concrete block of the same size and quality as for T-stub in tension was used for this test. Measurements were taken at four corners of the plate and at both ends of the bar, see Fig. 3. The measured curves can be found on Fig. 3. No collapse of the test specimen was achieved.

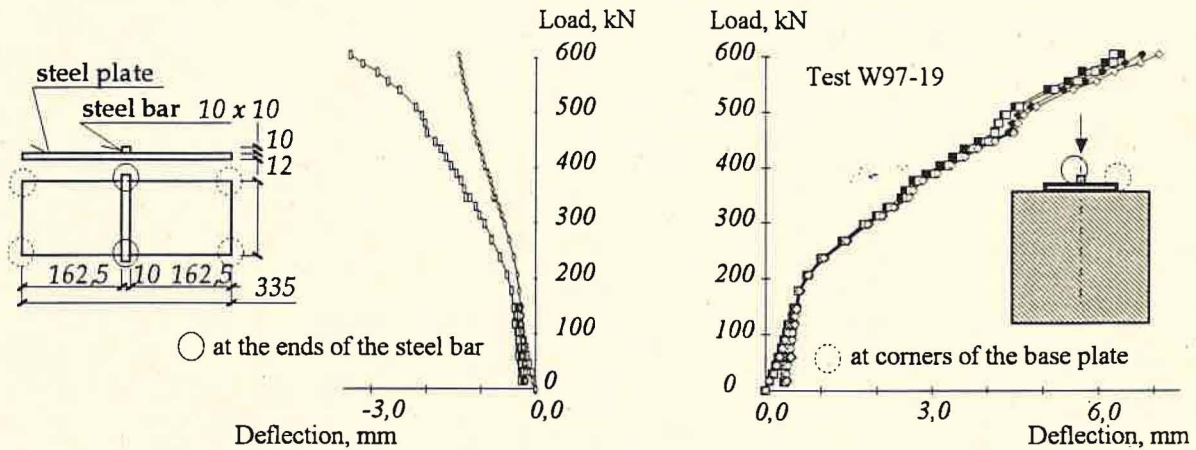


Fig. 3 Load-displacement curves of test of base plate T stub in compression, at corners of the base plate and at the ends of the steel bar [23]

4 COMPONENT SIMULATION

Modelling of the whole joint is complex due to the different deformability of the joint parts. The accuracy is mostly affected by the only one component. Therefore, modelling of the components is necessary to provide before solving of the whole joint. Separate modelling of components with different behaviour makes the work much easier and the modelling can be focused on few specific problems.

The basic components of the column base joint are the T-stub in compression and the T-stub in tension. The T-stub in compression represents compressed part of the column base joint where the load is transferred from the column flange to concrete block by bearing of the base plate. Development of contact zones is the main modelling problem of this component. The T-stub in tension represents the base plate anchored to the concrete block by anchor bolts. Modelling of anchor bolt, base plate in bending and contact of the parts of the joint are the main topics.

This following calculation shows behaviour of base plate in compression with different loading conditions. It represents a deformable base plate adjacent to a rigid plate under the column. The research was focused on investigation of the base plate deformation with variable position of the neutral axis.

The calculation was carried out using the code ANSYS 5.3. The model uses eight nodes brick elements SOLID 45 for the steel plate and SOLID 65 for the concrete block. The model enables plasticity of the steel and three dimensional behaviour of the concrete. 3D point-to-point contact elements CONTAC 52 were used at concrete-steel interface.

An infinitely long concrete block was considered for this calculation and therefore, only one layer of brick elements was used. The structure exhibits a two dimensional behaviour (in-plane strain) which requires applying of symmetric boundary conditions. With this approach, 3D non-linear behaviour of the concrete including cracking and crushing can be incorporated into two dimensional

model, see Fig. 4 for finite element mesh. Note that the supports are not displayed on the picture.

Numerical simulation of the test W97-03 was carried out to obtain additional data to evaluate the equivalent height of the joint for analytical prediction in elastic stage only. Because of symmetry, only one quarter of the experiment was modelled.

Point-to-point contact elements were used to model the steel-concrete interface. No friction between the concrete block and the steel plate was assumed. The model was loaded by deformation in the central part of the plate. Deformed shape of the model is included in Fig. 4. Fig. 5 shows principal stresses in the concrete with the steel plate removed and minimal i.e. compressive stress under the plate.

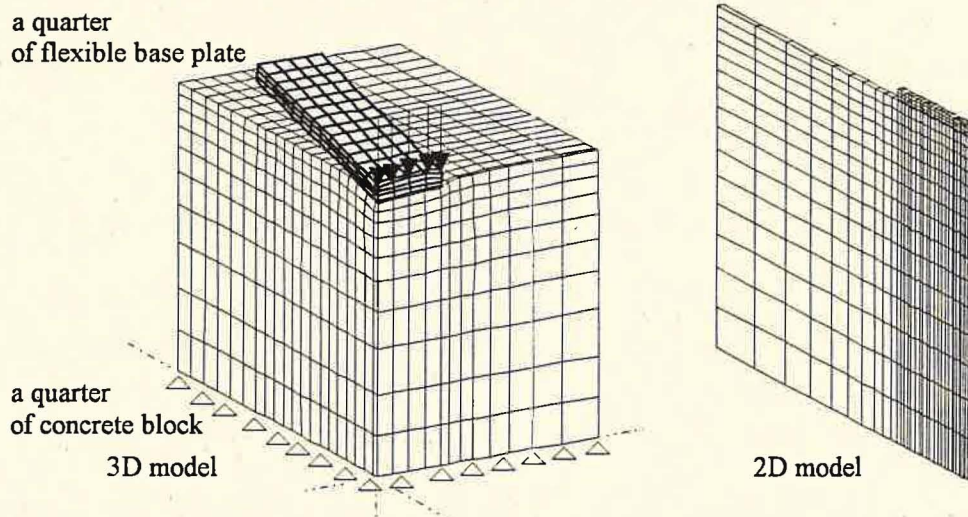


Fig. 4 The T-stub in compression loaded by deformation, the deformed mesh of the finite element model 3D model, 2D mesh for simplified solution

The other picture shows maximal i.e. tensile stress which developed mainly at the concrete surface adjacent to the contact area. The scale of the tensile stress is ten times smaller than the compressive stress.

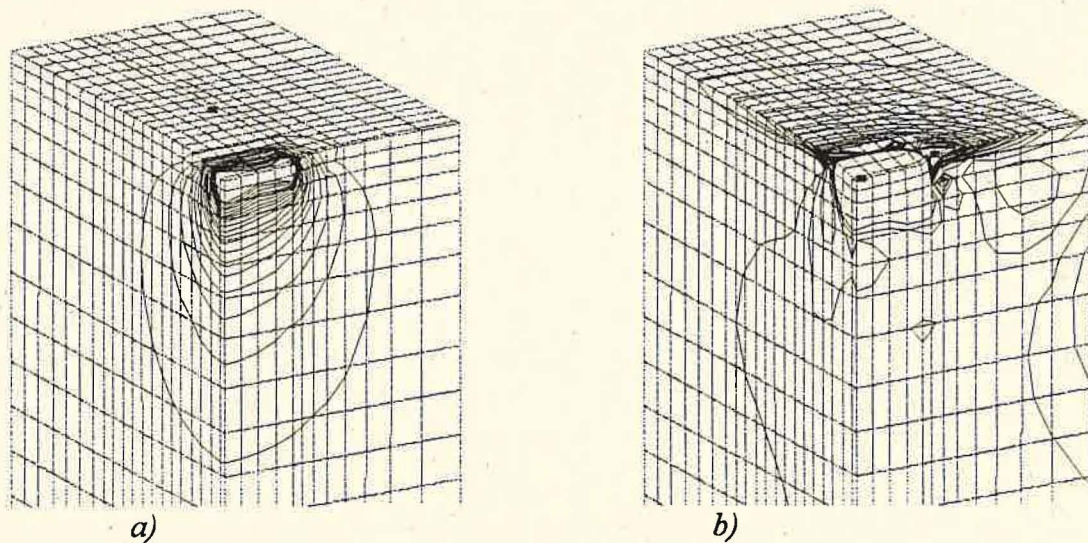
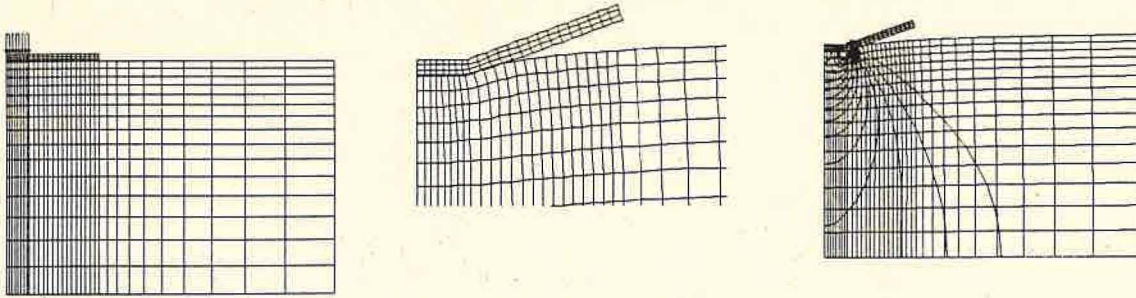
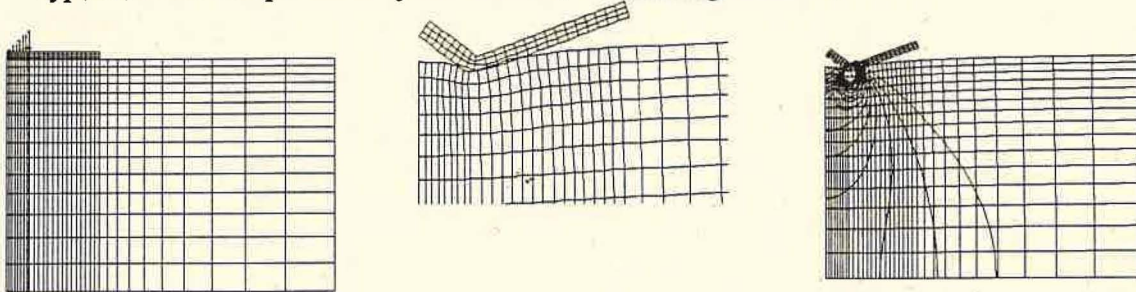


Fig. 6 Principal stresses in the concrete, a) compressive stress, b) tensile stress.

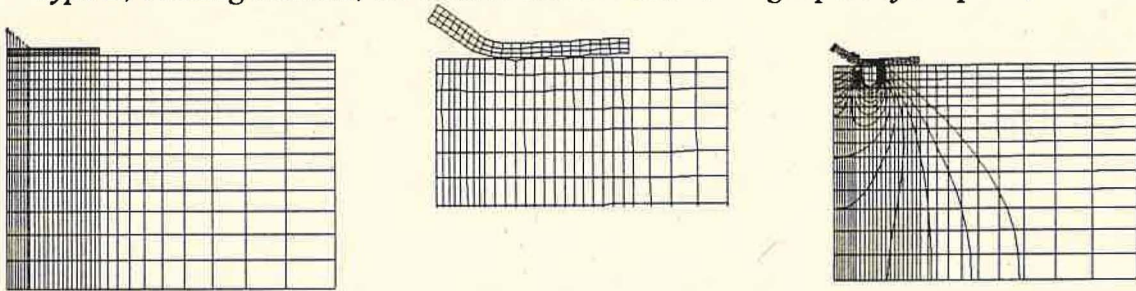
Position of the neutral axis was introduced by the loading. Prescribed displacement loading was applied on the rigid plate as shown on Fig. 6.



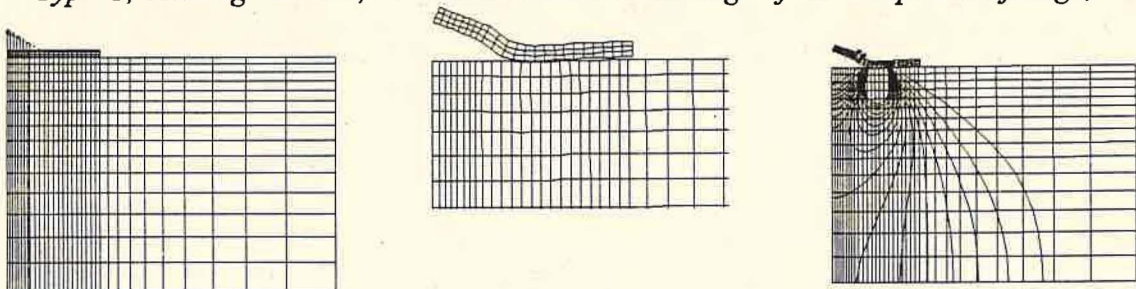
Type A, axial compression of the column, no bending moment,



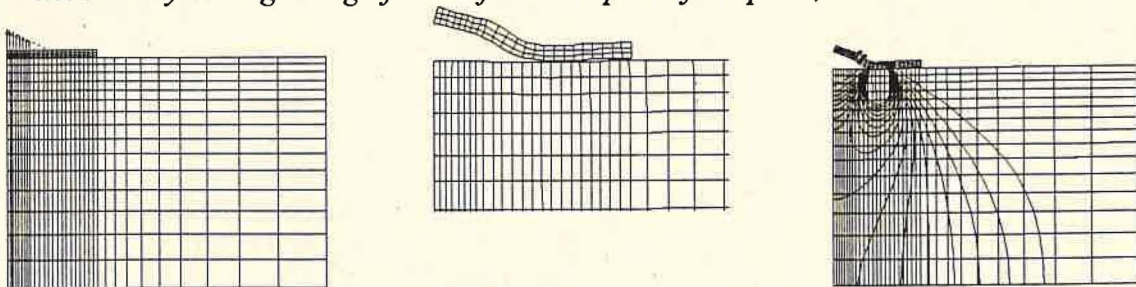
Type B, bending moment, the neutral axis is within the rigid part of the plate,



Type C, bending moment, the neutral axis is at the edge of the compressed flange,



Type D, bending moment, the neutral axis is 20 mm from the rigid part to the right, i.e. already on beginning of the deformable part of the plate,



Type E, bending moment, the neutral axis is 40 mm from the rigid part to the right, i.e. relatively far on the deformable part of the plate.

Fig. 6 Finite element model of T sub in compression and bending; different loading cases, deformed base plate in detail, and distribution of stresses in vertical direction

Five types of loading were considered: Type A, axial compression of the column, no bending moment, Type B, bending moment, the neutral axis is within the rigid part of the plate, Type C, bending moment, the neutral axis is at the edge of the compressed flange, Type D, bending moment, the neutral axis is 20 mm from the rigid part to the right, i.e. on the deformable part of the plate, Type E, bending moment, the neutral axis is 40 mm from the rigid part to the right, i.e. on the deformable part of the plate.

The work shown here represents only a part of an extensive study, Ref. [23]. The calculation was carried out with three different plate thickness 10 mm, 15 mm and 30 mm. Variable concrete quality from C12 to C45 was assumed. Fig. 6 shows results for 15 mm thick plate and concrete quality C30.

The analytical prediction of the anchor bolt elongation is sensitive to the prediction of the stress distribution along the anchor bolt, see Fig. 7. A special simulation of this subject shows small importance of modelling of a contact surface quality, the surface between bolt and the concrete block, under the elastic deformations and high influence under the loading close to the collapse. The model was calibrated against the tests of the embedded cast-in-situ anchor bolt with stiffened headed plate, see [13]. The main output, which can help in prediction model of the elongation - slip of the embedded part of the bolt, was the development of the stresses during the loading in elastic stage are presented in Fig. 8. The sensitivity study was steamed to the anchor bolt length and the headed plate influence on the elastic deformation at the concrete surface [28].

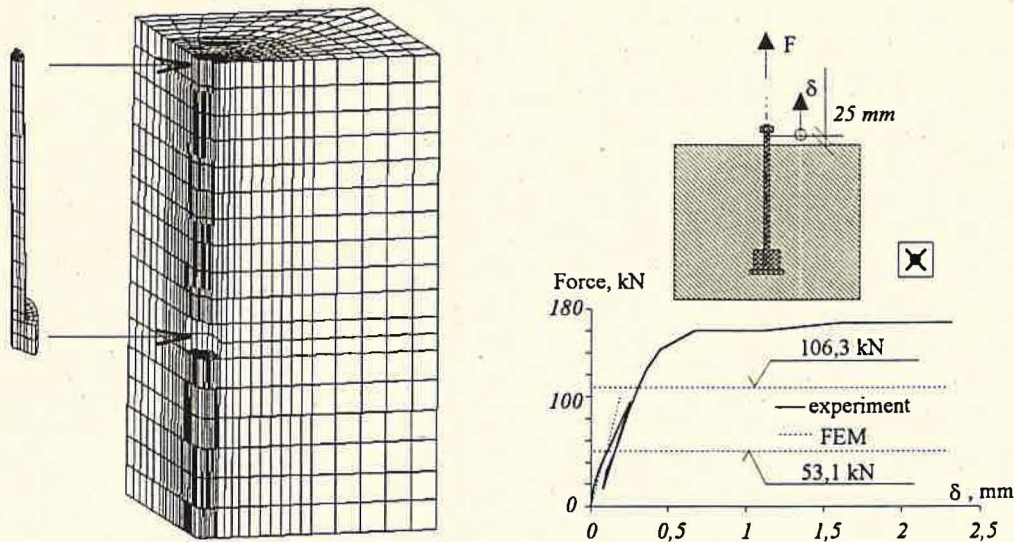


Fig. 7 The FE mesh for simulation of the anchor bolt, a quarter of the specimen, see test [13], bolt is glued by the contact elements (point to surface)

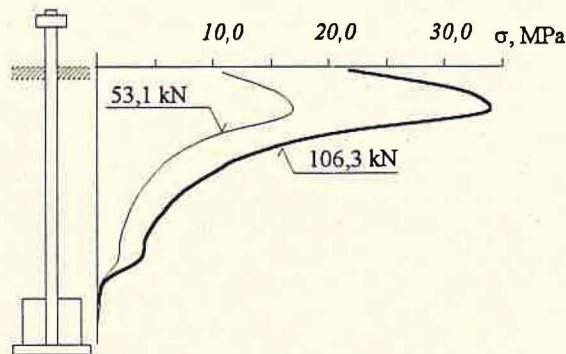


Fig. 8 The development of the contact vertical stresses during the loading

5 TWO DIMENSIONAL MODELS

5.1 Column Base with Base Plate

The described 2-D modelling technique is herein applied in order to simulate the behaviour of the base plate connection shown in Fig. 9. The steel column base connection consists of an RHS 120/200/10 steel column which is connected to a concrete block through a steel plate. The thickness of the base plate is considered as a critical parameter which varies taking the following values: *20mm*, *25mm* and *30mm*. Also six *M20- 5.6* bolts are used. The connection is simulated by means of a 2-D finite element mesh (Fig. 9) consisting of 4044 nodes and 2829 plain stress quadrilateral elements. The thickness of the plain stress elements are properly adjusted in order to take into account the three-dimensional properties of the structure compare [19]. Note that on the region of the holes of the plate, the plate and the bolt are overlapping. The interaction between the two bodies is taken into account by considering unilateral contact conditions between them. Unilateral contact conditions, are also assumed to hold between the plate and the concrete block. Elastoplastic stress-strain law for the steel profile and the plate is assumed to hold. A similar diagram is used to describe the material of the bolt. The material of the concrete block is considered as linear with modulus of elasticity $E_c = 29 \text{ GPa}$.

The model joint is loaded by applied displacements introduced as a sequence of 50 increments on the top of the edge of the column. At each increment, a displacement of *2 mm* is applied into the structure. Three groups of solutions are distinguished, each one corresponding to the three above mentioned plates with different thickness. In each set, the axial compressive loading of the connection consists of the following six cases: *0 kN*, *100 kN*, *200 kN*, *300 kN*, *400 kN*, *500 kN*. From each group, moment-rotation curves are obtained which are compared separately, but as well as totally.

From the first set of results for base plate thickness $t = 20 \text{ mm}$, notice that very quickly a contact zone is established under the right end of the base plate. The resting part of the plate starts separating from the concrete foundation, tensioning the left bolt. The deformation of the base plate decreases for increasing axial force. The reduction of the deformation of the base plate, is followed with decreasing of its plastic strains. The opposite situation occurs for the column which develops greater plastic strains with the increasing of the axial force. It is obvious that the increasing of the axial force acts beneficially for the base plate, decreasing its plastic strains. This failure occurs, due to the fact that as the plate arises it causes tension at the left bolt, thus creating an additional critical member failure. From the deformed shapes it is observed, that the larger part of the base plate for the first 20 increments is in contact ($N = 300 \text{ kN}$) with the concrete. For the following increments, as the base plate uplifts, only the left edge node and the base plate nodes near the right bolt remain in contact with the concrete foundation. This contact area increases along with the axial loading from *0* to *500 kN*.

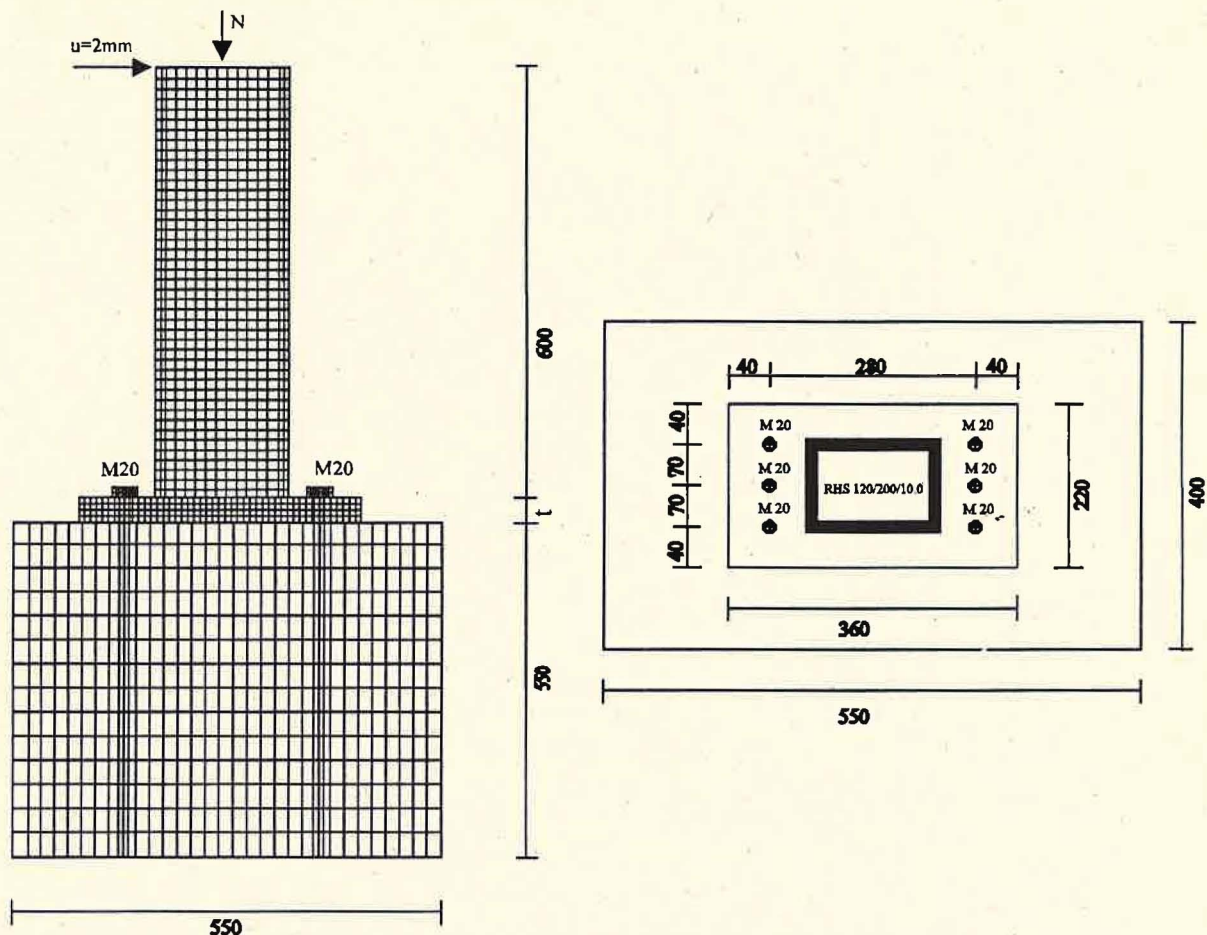


Fig. 9 Base plate connection the two dimensional example of calculation

Concerning the stress concentration on the joint, although the right region of the column and the base plate are naturally the first expected failure areas, similar stresses are developed in the left region after the 14th - 18th increment. This phenomenon occurs because of the prying forces which are developed in this area, when the left edge of the base plate comes in contact with the concrete base. For each case of axial load, the base plate for the first 10 - 18 increments separates from the concrete base in an area which extends, from the left edge of the plate to a certain point near the middle of the plate. For the following increments, the deformed shape of the base plate has as a result the contact of the left edge of the plate with the concrete base. This phenomenon creates through all the cases of axial load, a plastic area in the left region of the connection which develops similar final plastic strains with the right region. From the moment - rotation curves it becomes obvious that the moment capacity of the connection increases along with the increasing of the axial force. For axial force 0 kN, the moment capacity is near 90 kNm. In the case of 500 kN, the moment capacity reaches 116 kNm. In Fig. 10, the differences between the six cases of axial loading are clearly observed. Concerning the results obtained for base plate with thickness $t = 25 \text{ mm}$, the stress condition, as well as the plastic strains fields do change because prying forces are not present in this case. This results obtained are logical, since the stiffness of the base plate increases for thickness $t = 25 \text{ mm}$, permitting smaller deformability and reducing its final plastic strains. This fact is also observed from the maximum node detachment of the base plate at the left edge of the base plate.

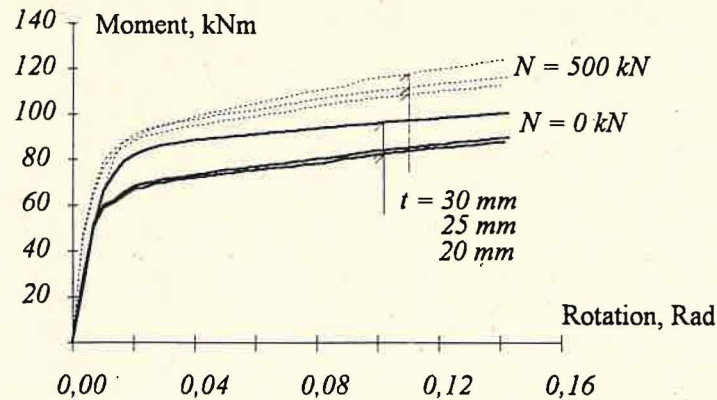


Fig. 10 Moment-rotation diagrams for various axial loads and base plate thickness ($t = 20, 25$ and 30 mm)

The steel column for each case of axial force, fails around the area of its right foot near the 40th increment, with stresses that exceed its ultimate strength. The stresses appearing in the left region of the base plate are beneath its ultimate strength. This occurs because the prying forces which were developed in the previous analysis for plate thickness $t = 20$ mm do not appear.

Through the deformed shapes of the base plate for the six cases of axial loading at increments 10, 20, 30, 40, 50, we notice the different response the connection exhibits in comparison with the connection of plate thickness $t = 20$ mm. The nodes of the base plate, have detached from the concrete foundation in an area that extends from the left edge of the plate reaching near the right bolt. We also observe that the bending of the base plate, is reduced in comparison with base plate of 20 mm thickness. This proves that the increasing of the stiffness of the base plate, affects significantly its response under the applied axial loading and bending moment combination. For axial force 0 kN, the base plate reaches first its ultimate plastic strain. The left bolt exceeds its yield strength, as the base plate uplifts causing tension on it. The bolt develops stresses near 380 N/mm^2 adding a critical failure of the left bolt. For axial force 100 kN, the ultimate plastic strains are developed at the same time at the plate and at the column. The left bolt in this case develops stresses near 362 N/mm^2 failing due to the tension forces that the plate transfers. Finally, for axial forces from 200 kN - 500 kN the column begins to be plastified from the outer to the inner parts. From the moment -rotation curves we notice that the moment capacity of the connection increases along with the increasing of the axial force. In Fig. 10, the obtained moment-rotation curves for the six cases of axial load are compared each other. Increasing the base plate thickness, the stiffness that it possesses permits limited deformation.

As a result, the base plate does not fail for any case of axial load. Significant stresses are developed mainly at the area of the right foot of the column, which fails first exceeding its ultimate plastic strain. It can be noticed that the bending of the base plate is limited and is slightly visible only for the last increments. Through all the cases of loading, the column fails after the 40th increment. The developed plastic areas create a plastic hinge at the lower right part of the steel column. Thus, the collapse of the structure occurs due to the plastification of the steel column and the other parts of the connection are not critical.

5.2 Embedded Column Base

The anchoring of the structural steel frame is possible to provide by embedded of the column footing in concrete. The improvement of prediction model of this connection was based on experimental program and on FE simulation [21].

When the model was successfully calibrated a wider range of sensitivity studies were conducted. This has provided satisfactory data for the establishment of the design model. The numerical modelling and was conducted by using the finite element code SBETA [11]. The program SBETA is a special finite element package for concrete problems 2D simulation. It has strong function to model the crack progression and descending branch of the load deflection curve. This is important for obtaining information about failure mode. The concrete properties modelling is important for the program includes non-linear behaviour in the compression including softening, crack generation in the compressed concrete, bi-axial criterion for crack geneses, decrease of the compressive stress and shear rigidity after crack initiation. The two dimensional, non-linear analyses were used. The load was applied by deformation. It is element with four nodes with Gauss integration points were used for modelling concrete and steel. The elements modelling the concrete base had the material properties shown on Fig. 11.

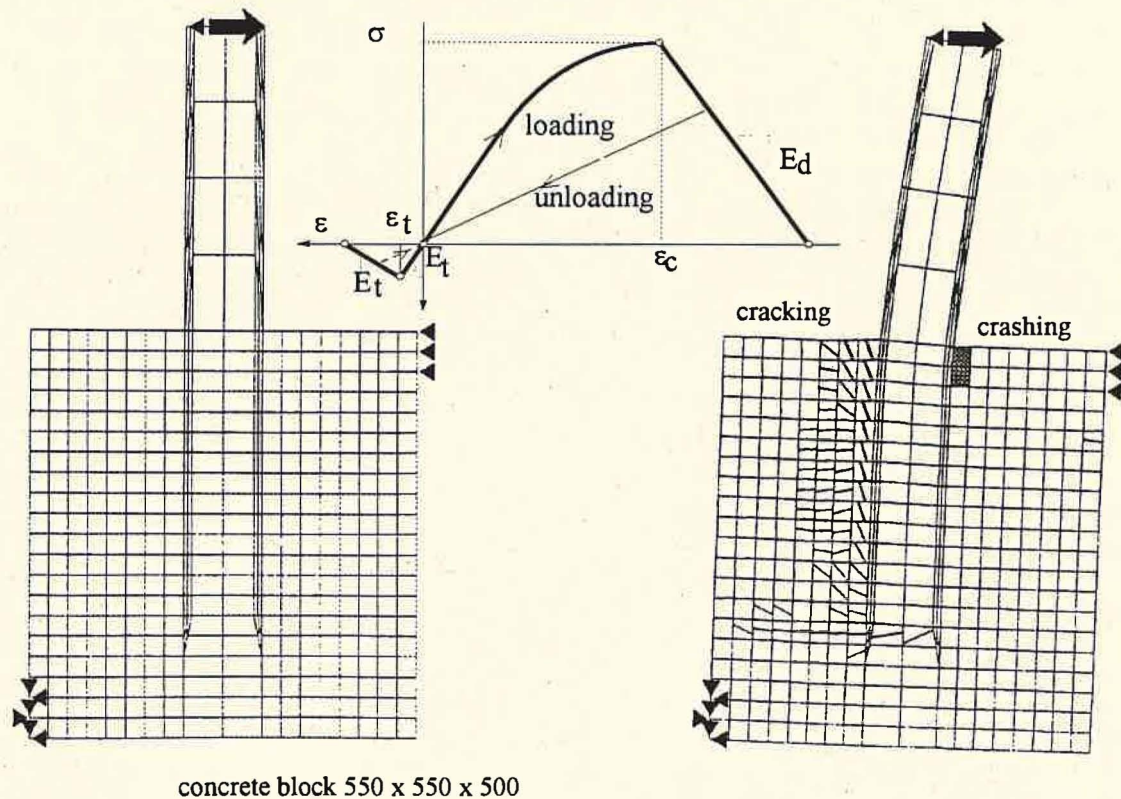


Fig. 11 The influence of the cracking of the concrete block on the embedded depth; material properties of the concrete elements, deformed shape including element cracking the last step before the collapse

In order to eliminate the error of two dimensional modelling, the finite element model was calibrated on the experimental results. The thickness of concrete element was changed in order

to achieve the same resistance of the model as the experiments. The resulting thickness was 765 mm instead of original 550 mm.

The FE simulation was streamed to observe the participation of the second flange, behaviour of the end plate embedded into concrete and the stress distribution in the concrete alongside the column loaded by moment and horizontal force. The high influence of the boundary condition was observed. The model represents the most unfavourable case of possible conditions, see Fig. 11.

Comparing the stress distribution of with different embedded depth, the following influence of the embendment depth can be observed. In the case of the embendment height $3,5*d_c$ the stress in concrete along the lower part of the steel column vanish due to the column flexibility. The stress main direction in concrete alongside the column flanges varies from the horizontal direction depending on the position and depth of embendment, see Fig. 12. As a result, the horizontal stress is in average 60% of the maximum concrete stress resistance.

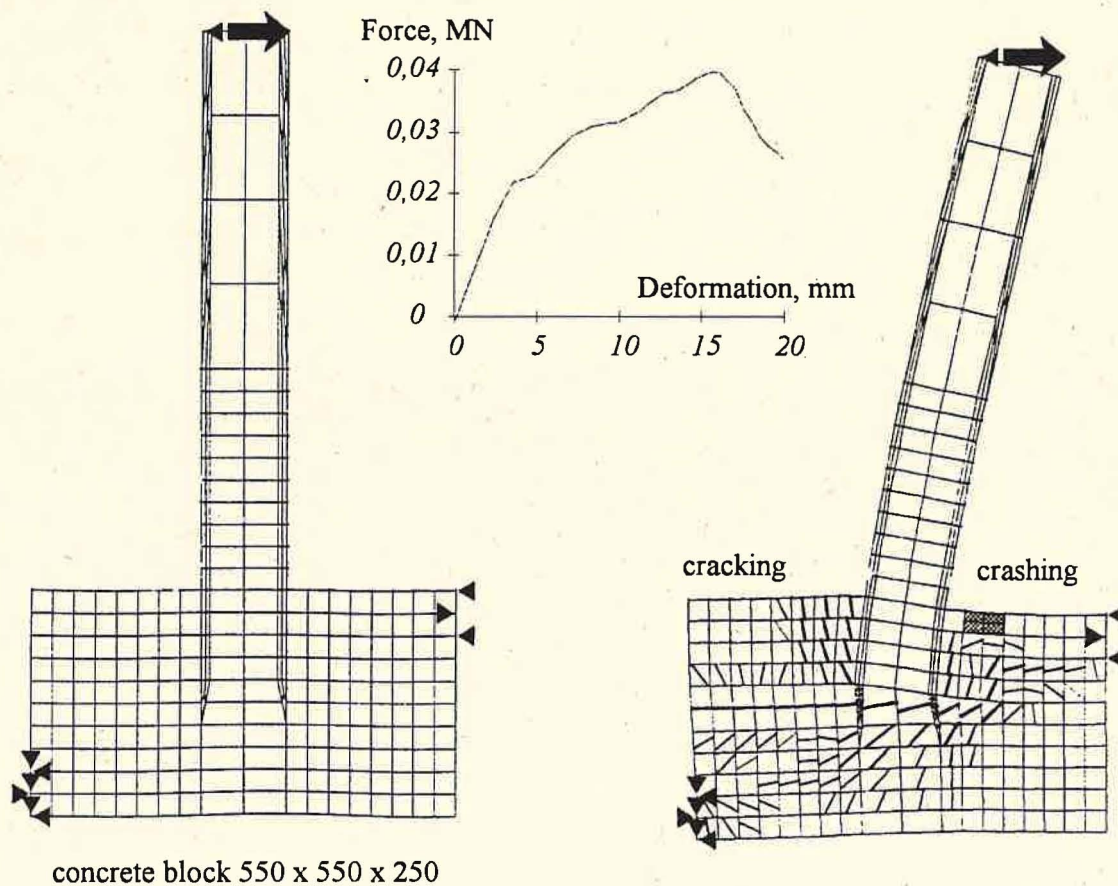


Fig. 12 The influence of the cracking of the concrete block on the embedded depth; deformed shape including element cracking the last step before the collapse; force - deformation diagram, the concrete cracking and the unloading part of the curve shows the non-linear influence of the material

6 CONCLUSIONS

- The FE simulation allows for the simulation the column base behaviour with good accuracy in initial stage of loading . The accuracy decreases in the non-linear part of the load deformation curve and the simulation of deformational capacity is a difficult task similar to experimental observations in this case of very high forces and very low deformations due to high loads.
- The present state of the hardware and software informatic support of the FE simulation enables to prepare a sensitivity study of different problem, but is limited for use in practical design to special particular problems. The solid 3D models are limited by very high number of freedom, but 2D models are applicable to study a particular special problems.
- The FE models checked to experiments are important tool for understanding the stress distribution during the loading, in positions where is impossible provide the direct measurement.
- Modelling of the whole joint is complex due to the different deformability of the joint parts. The accuracy is mostly affected by the only one component. Therefore, modelling of the components including their particular needs as contact, friction, concrete cracking and so on is necessary to provide before solving of the whole joint.
- For the evaluation of the simulation models a special tests are necessary to run with additional measurements of tests data compare to needs for check of the traditional technical models.
- The particular problems are efficient to study by two dimensional solution only based on calibration of the depth to the experiments.

Acknowledgement

The presented work has been carried out at Aristotle University of Thessaloniki and at Czech Technical University. The authors acknowledges with thanks the financial support by the Greek Secretariat for Research and Technology (PENED-95:1748 *Structures with semirigid connections: Development of software for static and dynamic computation*) and by Czech Ministry of Education (Grant COST C1-10 *Semi rigid behaviour of structural connections*). The authors would like to thank Mr. J. Pertold and Mr. J. Mareš for help with preparation of the materials for this document.

REFERENCES

- [1] Ádány S., Dunai L., *Rigidity of Column-Base Connections under Combined Loading*, Preliminary Report of the International Colloquium, European Session, Stability of Steel Structures, ed. Iványi M., Veröci B., Vol. 2, Budapest, pp. 3-10. (1995).
- [2] Balakrishnan S., Murray W., *Concrete Constitutive Model for NLFE Analysis of Structures*, Journal of Structural Engineering, Vol. 114, No. 7. (1987).

- [3] Balogh J., Iványi M., *Parametric Study of Column-Base Connections*, Preliminary Report of the International Colloquium, European Session, Stability of Steel Structures, ed. Iványi M., Veröci B., Vol. 2, Budapest, pp. 11-16. (1995).
- [4] Baniotopoulos C. C., *On the Numerical Assessment of the Separation Zones in Semirigid Column Base Plate Connections*, Structural Engineering and Mechanics, No.2, (3), pp. 295 - 309. (1994)
- [5] Baniotopoulos C. C., Karoumbas G. Panagiotopoulos P. D., A contribution to the analysis of steel connections by means of quadratic programming techniques. In: *Proc. 1st Europ. Conf. on Numer. Meth. in Engng.*, pp. 519-525, Amsterdam: Elsevier (1992).
- [6] Baniotopoulos C. C., On the numerical assessment of the separation zones in semirigid column base plate connections. *Struct. Engrg & Mech.* 2, 1-15. (1994).
- [7] Baniotopoulos C.C., On the separation process in bolted steel splice plates. *J. Construct. Steel Res.* 32, pp.15-35. (1995).
- [8] Baniotopoulos C.C. and Abdalla K.M., Steel column-to-column connections under combined load: A quadratic programming approach. *Comput. Struct.* 46, pp.13-20. (1993).
- [9] Bortman J., Szabó B.A., *Nonlinear Models for Fastened Structural Connections*, Computers & Structures, Vol. 43, No. 5., pp. 909-923. (1991):
- [10] Bortman J., Szabo B.A., Nonlinear models for fastened structural connections. *Comput. Struct.* 43, pp. 909-1023 (1992).
- [11] Cervenka V., Eligehausen R., Pukl R., (1991): *SBETA Computer Program For Nonlinear Finite Element Analysis Of Reinforced Concrete Structures*, Institut für Werkstarre im Bauwesen, Universität Stuttgart. Dunai L., Adany S., Wald F., Sokol Z., *Numerical Modelling of Column-Base Connections, Computational Techniques for Structural Engineering*, in Civil, Comp. Press, Edinburg, pp. 171 - 178, ISBN 948749-45-8. (1996):
- [12] Jaspart J. P., Bursi O. S., Benchmarks for finite element modelling of bolted steel connections, University of Trento (1990).
- [13] Kalfas C., Pavlidis P., Galoussis E., Inelastic Behaviour of Shear Connection by a Method Based on FEM, *J. Construct. Steel Res.* 44, 107 - 114, (1997).
- [14] Kontoleon M. J., Mistakidis E. S., Baniotopoulos C. C., Panagiotopoulos P.D, Parametric analysis of the structural response of steel base plate connections. *Comput. Struct.* (1998).
- [15] Krishnamurthy N., Graddy D.D., Correlation between 2- and 3-dimensional finite element analysis of steel bolted end-plate connections. *Comput. Struct.* 6, pp. 381-389. (1976).
- [16] Krishnamurthy N., Thambiratnam D.P., *Finite Element Analysis of Column Base Plates*, Computer & Structures, Vol. 34, No. 2, pp. 215-223. (1990).
- [17] Krishnamurthy N., *FEABOC - Finite Element Analysis of Bolt Connection*, Proc. Eighth Conference on Electronic Computation, Am. Soc. Civ. Engrs., pp. 312-325. (1983).
- [18] Lafraugh R.W., Magura D.D., *Connection in precast concrete structures-column base plates*, Journal of Prestressed Concrete Inst., Vol. 2, pp. 18-39. (1966).

- [19] Mistakidis E. S., Baniotopoulos C. C., Bisbos C. D., Panagiotopoulos P. D., A 2-D numerical method for the analysis of steel T-stub connections. *Proc. 2nd Greek Conf. on Computational Mechanics*. Chania 1996, pp. 777-748. (1996).
- [20] Mistakidis E. S., Baniotopoulos C.C., Panagiotopoulos P. D., A numerical method for the analysis of semirigid base-plate connections. *Proc. ECCOMAS 96*, J.Wiley & Sons Ltd, pp. 842-848. (1996).
- [21] Panagiotopoulos P. D., *Inequality Problems in Mechanics and Applications. Convex and Nonconvex Energy Functions*. Boston-Basel Birkhauser (1985).
- [22] Pertold J. *Steel Column Embedded in Concrete Foundation in Czech, (Pripojení ocelového sloupu k základové konstrukci zabetonováním)*, Ph.D. thesis, ČVUT Prague (1996).
- [23] Schwarz M., Flexible plate on concrete support (in Czech), *Diploma Thesis*, ČVUT Prague (1997).
- [24] Sokol Z., Wald F., *Experiments with T-stubs in Tension and Compression*, Research Report, ČVUT, Prague, (1997).
- [25] Thambiratnam D.P., Krishnamurthy N., Computer analysis of column base plates. *Comput. Struct.* 33, 839 - 850, (1989).
- [26] Wald F., Villanova F., Zühlke A., *2D and 3D Modelling of a T-stub, the COST C1 Example*, v COST C1 No. 97/WG6/6, Munich, p. 1 + 8. (1997)
- [27] Wald F., *Patky sloupu, Column Base*, VUT, Prague, ISBN 80-01-01337-5, p. 137. (1995).
- [28] Wald F., *Column-Base Connections*, A Comprehensive State of the Art Review, ČVUT Prague, p. 112. (1993).
- [29] Wald F., Obata M., Matsuura S., Goto Y., *Flexible Baseplates Behaviour using FE Strip Analysis*, Acta Polytechnica, ČVUT Vol. 33, No. 1, Prague, pp. 83 - 98, (1993).

GUIDELINES FOR A NUMERICAL MODELLING OF BEAM-TO-COLUMN MINOR-AXIS JOINTS

Luís Neves

University of Coimbra, Portugal

Fernando Gomes

University of Coimbra, Portugal

In a beam-to-column minor-axis joint, the beam is directly connected to the column web. The deformation of the web, the deformation of the connecting elements (end plate, cleats, bolts), are responsible for the rotation of the joint, and define the moment-rotation ($M-\phi$) curve. In Eurocode 3, rules for evaluating the $M-\phi$ response of all the connecting elements are available. However, the behaviour of a minor-axis joint cannot be predicted because there are not rules available to define the $M-\phi$ curve of the column web. In this paper a numerical model of the column web in a minor-axis joint is described. This model has been validated with theoretical solutions and laboratory tests. The aim is to identify the relevant parameters and the general options that should be taken, thus giving the reader guidelines for modelling similar problems.

INTRODUCTION

In a steel frame, beam-to-column joints are neither pinned or fully-rigid; their real behaviour is characterised by a non-linear moment-rotation ($M-\phi$) curve - Figure 1. Modern design codes allow the designers to account for this fact in the structural analysis and design, leading to an higher accuracy and economy. However, to perform such an analysis the designer has to know the $M-\phi$ curve of the joint or, at least, some of its characteristics. These may be derived from laboratory tests, validated numerical simulations or from analytical models like the available in Eurocode 3 - annex J. From these methods, the most suitable for practical design is the application of analytical models, for reasons of economy, time and complexity. The analytical model adopted by Eurocode 3, the "Component method", is widely accepted by scientific community and used by designers. Its philosophy is simple: for a given connection, the sources of deformability are identified. Then, the available application rules give, for each of these components, the plastic moment (M_{pl}), the stiffness (S_j) and the rotation capacity (Figure 1). The global $M-\phi$ behaviour of the connection is then derived from a model that is an association of translational springs. From this flows that the scope of

this method may be extended to any type of joint, as far as we are able to characterise all the relevant components.

In a beam-to-column minor-axis joint, the beam is directly connected to the column web (Figures 1, 2 and 3). The total deformation is due to the deformation of the connecting elements and to the deformation of the column web, that is a plate subjected to bending and shear. Eurocode 3 gives application rules to characterise the behaviour of all components but one: the web of the column. Its scope is thus limited to the case when the two moments, acting on both sides of the column web (Figure 2) are symmetrical, becoming this joint a beam splice. In order to extend the scope of the "Component method" to the general case, a research program has been conducted, first at the University of Liège, Ref [2-4], and later at the University of Coimbra, Ref [5], [9-13]. This research program included the development of theoretical solutions, laboratory tests and numerical simulations, using two finite element packages - FINELG, Ref[6] and LUSAS, Ref [1]. [9-11].

More recently, we had the opportunity to continue this research at the University of Liège, during a COST mission, Ref [13]. Comparison of the models that we had proposed for evaluating the stiffness of minor-axis joints to laboratory tests and further numerical simulations with FINELG were made.

DEFORMATION OF THE COLUMN WEB

Figure 1 shows the typical moment-rotation curve of the column web in a minor axis-joint.

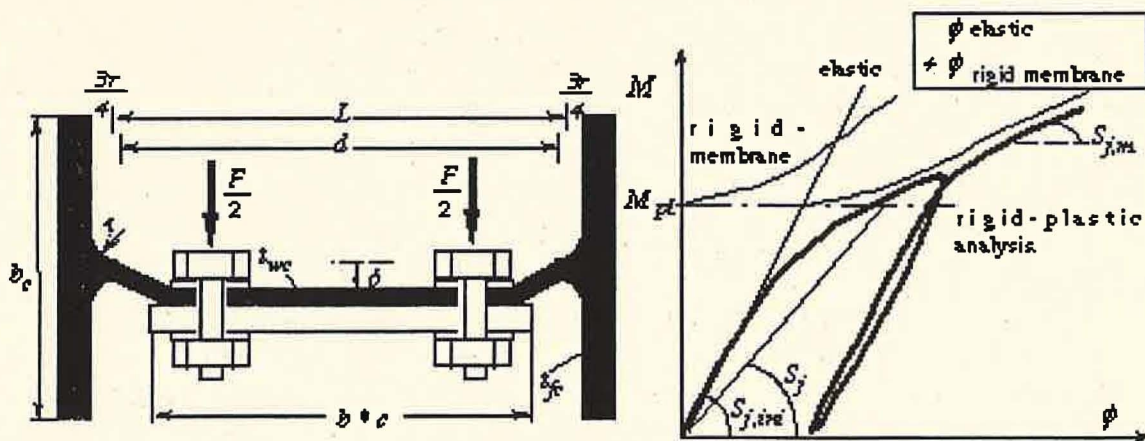


FIGURE 1: Geometric characteristics and typical behaviour of the column web in a minor-axis joint

At first, the behaviour is linear-elastic, and is characterised by the initial stiffness, $S_{j,ini}$. As yielding progresses, the stiffness decreases (at each level of loading the secant stiffness is S_j) and would tend, in a first order plastic analysis, asymptotically to zero as the moment approaches the plastic moment, M_{pl} . However, in this geometry of connection, the column web often presents a deformation out of the plan, δ , that is greater than its thickness, t_{wc} . As a consequence, the $M-\phi$ curve does not tend to

M_{pl} , but this level of moment will be exceeded by a post-plastic behaviour. This post-plastic $M - \phi$ curve is at first parabolic, then the stiffness stabilises at a constant value, the membrane stiffness, $S_{j,m}$.

This effect of overstrength has to be investigated, as if it is safe for the column web itself, it may be unsafe for the whole joint, causing brittle failure of connecting elements like bolts or welds. The plastic moment (and naturally the non-elastic $M - \phi$ curve) is always associated to a plastic mechanism. The possible plastic mechanisms have been established by Gomes, Ref [2], as well as the corresponding plastic moments, M_{pl} .

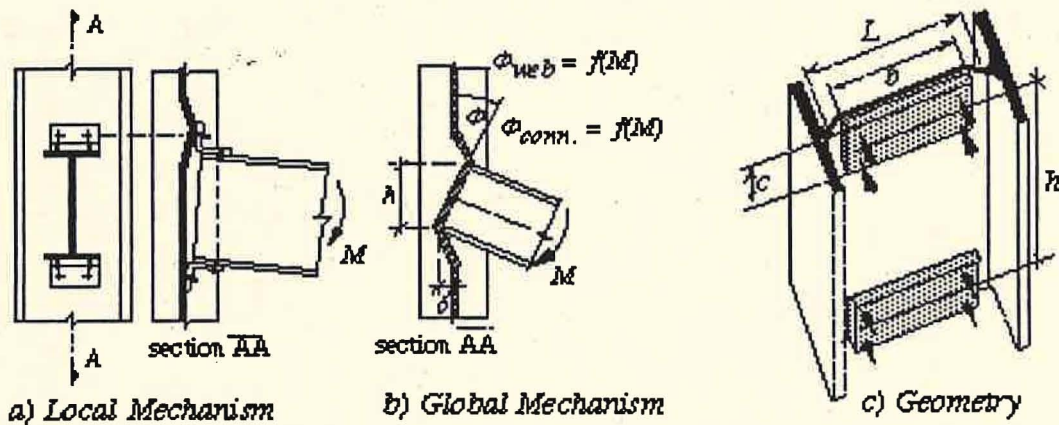


FIGURE 2: Types of yielding mechanisms and relevant geometrical parameters

PARAMETERS TO BE CONSIDERED

The relevant parameters that should be considered when modelling a column web in a minor-axis joint are:

Type of web's failure mechanism

This may be local, involving one of the forces composing the bending moment transmitted from the beam - Figure 2a; or global, involving the two forces - Figure 2b. Local mechanism occurs for large values of h - Figure 2b and c, and global mechanism for small values of h . Non dimensionally, this may be controlled by the parameter $\gamma = h/L$, and the boundaries between these two types of mechanisms have been established in Ref [2].

Dimensions $b \times c$ of the loaded area

These corresponds to the non dimensional parameters $\beta = b/L$ and $\alpha = c/L$ - Figures 1 and 2c. Both resistance and stiffness increase for larger loaded areas $b \times c$.

Slenderness of the column web

It is defined by the parameter $\mu = L/t_{wc}$ - Figure 1, that plays a fundamental role on the elastic and on the post-plastic behaviour of this joint component. For commercial hot

rolled sections of IPE and HE series, μ varies approximately between 10 and 50. If μ is small (10-15), then shear effects become important resulting in a smaller initial stiffness and possible failure by punching shear. The post-plastic behaviour of overstrength and membrane stiffness are neglectable for the out of plan deformations usually observed - Ref [11].

If μ is large (40-50), then shear effects are neglectable, and it is difficult to identify, from a test, the plastic moment, as the $M-\phi$ curve shows a very important influence of membrane effects. For intermediate values of the slenderness (μ between 15 and 40), it is important to account for shear, bending and membrane effects on the $M-\phi$ response of the column web.

Restraint of the column flanges to the web's rotation

Two situations have to be considered: tridimensional joint - Figure 3a, where major-axis beams prevent rotation of the column flanges. Column web may then be modelled as a plate clamped at the line connecting it to the flanges. The other situation is a minor-axis joint alone - Figure 3b, where the column flanges are free to rotate; their restriction to the web's rotation may be expressed by a parameter ψ , that results from the section geometrical characteristics - Figure 1;

$$\psi = \frac{\left(\frac{L}{t_{wc}}\right)}{\left(\frac{b_c}{L}\right) \cdot \left(\frac{t_{fc}}{t_{wc}}\right)^3} \quad (1)$$

where $\psi = 0$ models the clamped web. In the study that we have conducted, Ref [11-12], both values of $\psi = 0$ and $\psi = 22$ have been adopted to model, respectively, situations of Figure 3a and Figure 3b. This value of $\psi = 22$ corresponds to a safe low boundary of flange torsional stiffness, according to the variation of ψ in the range of commercial IPE and HE series.

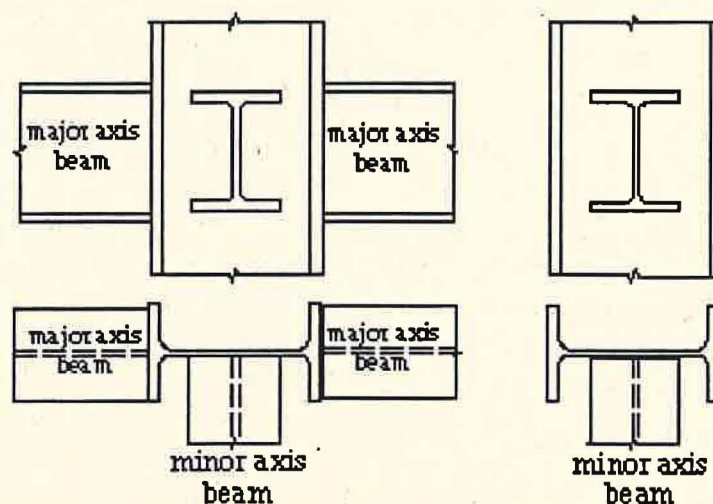


FIGURE 3: Tridimensional and minor-axis joints

To understand the behaviour of these joints, and to propose a model to evaluate their initial, secant and membrane stiffnesses, a parametric study involving all the parameters referred above, has been conducted - Ref [9-11].

Ranges of variation for the different parameters were: $0,08 \leq \beta \leq 0,75$, $0,05 \leq \alpha \leq 0,2$, $10 \leq \mu \leq 50$, $0,5 \leq \gamma \leq \infty$. Three types of analysis have been performed: elastic, elasto-plastic (due to material nonlinearity) and second-order elasto-plastic (due to both material and geometric nonlinearities). The conclusions of this study are published in Ref [11-12]. It involved more than 120 numerical simulations using the finite element package LUSAS, Ref [1]. Options taken and results given by the program, have been compared to available information from other studies, namely the numerical simulations performed by Gomes with FINELG, Ref [2].

FINITE ELEMENT MODEL

Finite Element Mesh

The most suitable element to model the column web is the thick shell. It leads to much lighter models than solid elements, and may cope with the relevant deformations: bending, shear and membrane. Naturally that if one wishes to model a situation where, due to an high slenderness of the web, shear effects are neglectable, one may use thin shell elements. On the other hand, if the slenderness is small ($\mu < 15$), second order membrane effects are neglectable, and it is quite accurate to use thick plate elements.

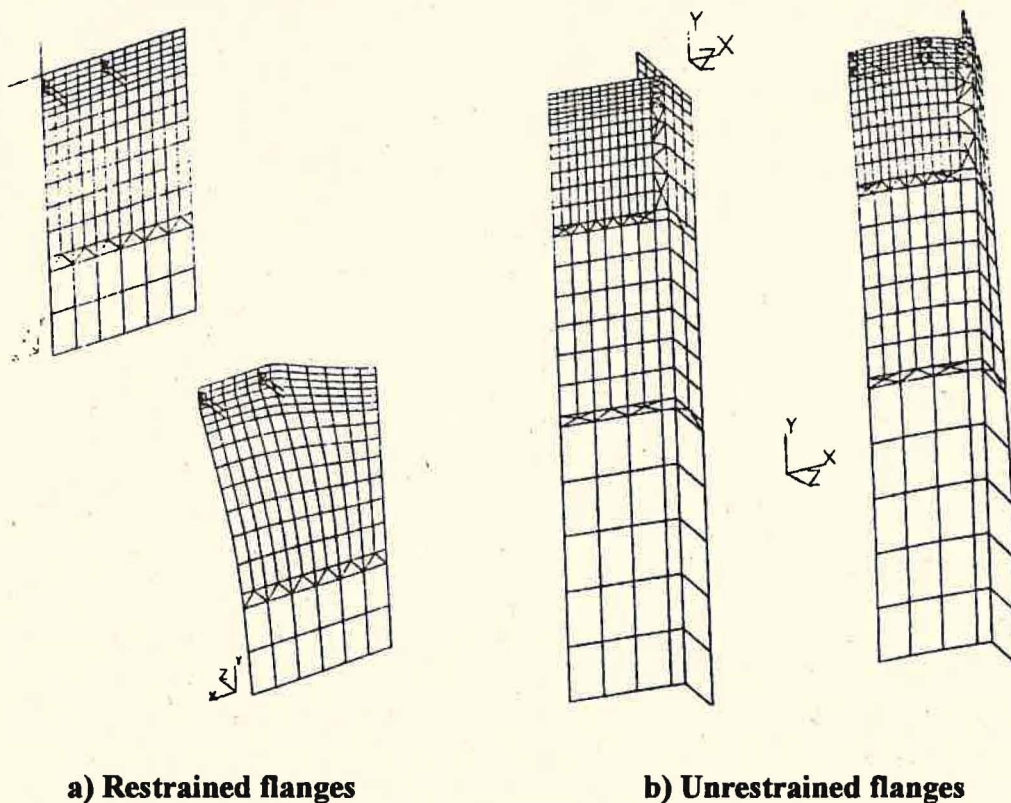


FIGURE 4: Finite element meshes for local mechanism

Some of the meshes adopted are represented in Figure 4. It is helpful to account for the symmetry of the joint, that may be observed in both directions x and y for local mechanisms, and thus modelling only one-quarter of the column. For modelling global mechanism the y -axis symmetry and the x - axis anti-symmetry may be used.

The meshes showed in Figures 4a and 4b model, respectively (and for the local mechanism) the situations of Figures 3a and 3b. In the Tridimensional joint the column web may be modelled as a clamped plate, but if the flanges may rotate, these have to be modelled as well.

Successive refinements of the meshes led to the adoption of 12 elements to model the half of the web in the x direction - Figure 4. Comparison of the plastic load (obtained from a first order plastic analysis) to the theoretical plastic load derived by Gomes, Ref [2], for different mesh densities are showed in Figure 5.

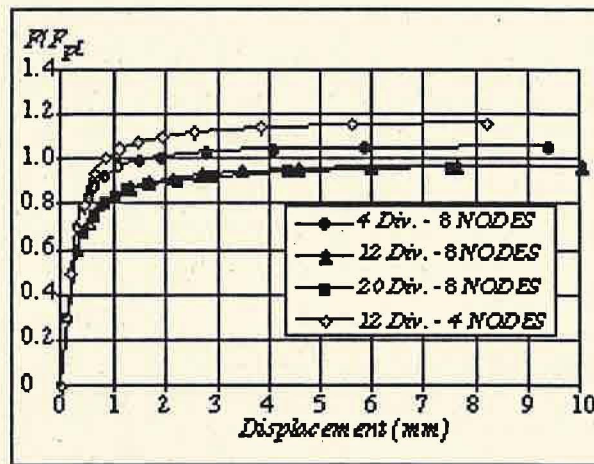


FIGURE 5a: Sensitivity to mesh density and element typology

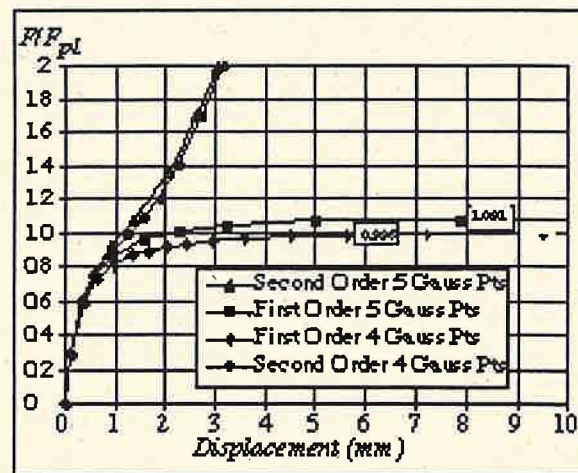


FIGURE 5b: Sensitivity to number of Gauss integration points

The type of element is of great importance. It was found that eight-noded thick shell elements should be adopted (instead of four-noded elements) in the zone of the plastic mechanism. In Figure 5a it is showed that having 4 eight-noded elements leads to an

higher accuracy than 12 four-noded elements. However, to save computation time, four-noded elements may be used in zones that do not affect the shape of the plastic mechanism, and where the mesh may be less refined - Figure 4. Transition between these zones of different mesh densities should be away of the loaded area (in the y direction) of, at least one half of the length of the column web in the x direction - Figure 4. Transition between different mesh densities may be done using three-noded triangular shell elements.

In LUSAS, quadrangular eight noded thick shell elements (QTS8) have the option of 4 or 5 Gauss integration points. This last option leads generally in these problems to stiffer solutions than the exact. This has been verified in our problem - Figure 5b.

Material Model

It is well known that steel has a stress-strain law characterised by a linear curve up to the yielding stress. Then, after some yielding strain hardening is observed. In a multiaxial stress field the yielding condition may be represented by the yielding surface. A suitable yielding surface for steel is the Huber-von Mises cylinder. Strain hardening may be neglected in these situations as it does not affect considerably the $F - \delta$ curve.

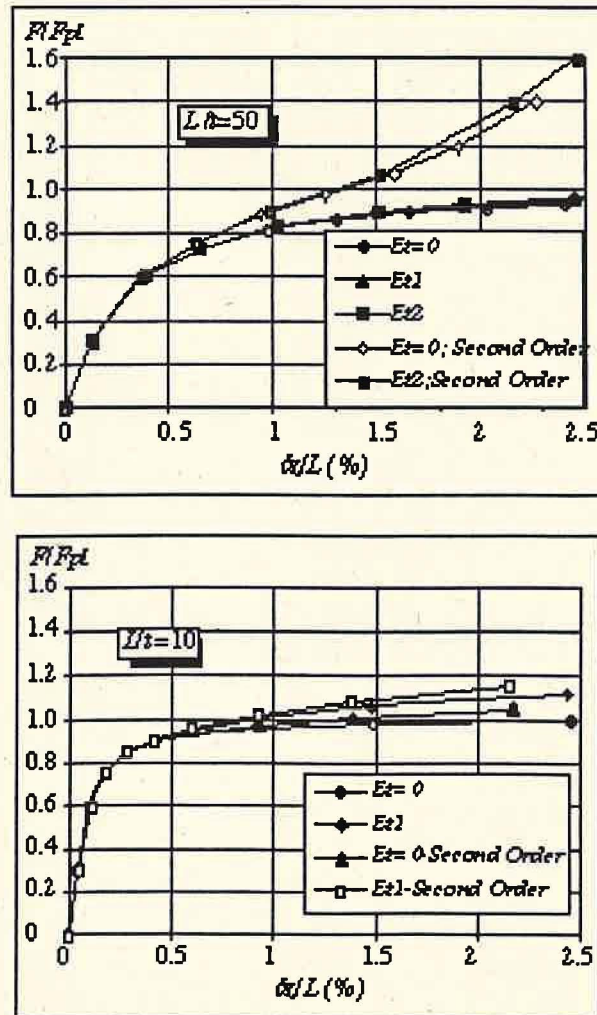


FIGURE 6: Strain hardening effect

Figure 6 shows the effect of strain hardening (a) for a slenderness of $\mu = 50$ and (b) of $\mu = 10$. The corresponding hardening modulus were $E_{t1} = 0,003E$ and $E_{t2} = 0,02E$. It is interesting to observe that for an high slenderness, curves with and without strain hardening are hard to distinguish. The same qualitative results have been published by Korol and Mirza, Ref [7] and Wardenier et al, Ref [8], for comparable situations of RHS joints.

Geometric Nonlinearity

The importance of second-order membrane effects referred in previous sections imposes a geometric nonlinear analysis. In Figure 6, for $\mu = 50$, the difference between geometric linear and second order analysis may be observed.

The total Lagrangian formulation, that takes the initial configuration of the structure as reference during all the solution procedure may be used.

Analysis procedures

Incrementation and iteration

In problems where nonlinearities are present, structural response has to be found by a load increment procedure (step by step). In the Newton-Raphson method, for each load increment, the residuals are eliminated by successive iterations, and in each iteration the structure is analysed with a reformulated stiffness matrix k_T and the applied loads are constant. Iterative procedure stops when equilibrium is reached, that is traduced by the satisfaction of the associated convergence criteria. This algorithm has a family of modified algorithms, that use, for each load increment a pre-specified number n of the stiffness matrix reformulations. The most common of these modified algorithms are those of $n = 0$ (initial stiffness method), $n = 1$ and $n = 2$. In our study we have concluded that, among these methods, the most efficient is the standard Newton-Raphson.

In these problems, as discussed in the previous sections, progressive yielding leads to a drop of stiffness that may be reduced almost to zero (Figure 6b). In such situations, the incrementation method referred above may not converge. One of the procedures to solve this problem is the arc length method; in each load increment, iteration procedure goes on with a variable load level, that follows a pre-specified path. In our study, we found that a very efficient procedure is the use of the standard Newton-Raphson method until the tangent stiffness of the structure becomes one-half of the initial stiffness. Then, solution proceeds with the arc-length method.

Convergence

On each load step, iterative procedure stops when all the convergence criteria are satisfied. Choice of these criteria has to be judicious, as they should be tight enough to guarantee sufficient accuracy and on the other hand slack enough to reduce computation time. We have found that the following criteria meet these conditions:

a) Euclidean Residual Norm - norm of the residuals ψ as a percentage of the external forces R_y

$$\gamma_{\psi} = \frac{\|\psi\|_2}{\|R\|_2} \times 100 \leq 0.1$$

b) Euclidean Displacement Norm - norm of the iterative displacements δ_a as a percentage of the norm of the total displacements a ;

$$\gamma_d = \frac{\|\delta_a\|_2}{\|a\|_2} \times 100 \leq 0.1$$

c) Work Norm - work done by the residual forces on the current iteration as a percentage of the work done by the external forces on iteration zero;

$$\gamma_w = \frac{(\psi^i)^T \delta_a^i}{R^T \delta_a^i} \times 100 \leq 0.1$$

Termination

If the number of load steps and the initial load level for each step are not specified, incrementation may proceed automatically until the satisfaction of convenient termination criteria. Suitable criteria for these problems are a maximum load factor and a maximum nodal displacement. The first governs in a second order analysis of a slender column web, and the second governs in a second order analysis of a thicker web or in a geometrical linear (first order) analysis.

VALIDATION OF THE NUMERICAL MODEL

Validation of the described numerical model was based upon comparison with three sets of results.

Qualitative comparison with other numerical models

Gomes, Ref [2] and Jaspert, Maquoi et al, Ref [6], for the same problem, Ting, Shanmugam and Lee, Ref [14] for joints between hot rolled sections and RHS, describe numerical models with similar characteristics to ours. In particular the mesh geometry and the adoption of thick shell elements are common aspects. Some of the studies were made with thin shell elements, but the slenderness of the plates studied justified so. Wardenier et al, Ref [8] refer as well the better results achieved with eight-noded elements, comparing to four-noded elements. The strain hardening effect on the behaviour of RHS joints is also neglected in their studies, after investigation of its importance.

From the above studies, qualitative conclusions that point in the same direction of ours, could be drawn; behaviour for large displacements, influence of the size of the loaded area, and slenderness, among others.

Comparison of the obtained values for F_{pl} with the corresponding theoretical values

All the plastic force values F_{pl} , obtained from first order finite element analysis, were compared with the corresponding theoretical values established by Gomes, Ref [2] and by Gomes, Jaspart and Maquoi, Ref [4]. In Ref [11] we could report the excellent correspondence observed. We refer in this paper that for the whole range of parameters studied, μ , β , α and γ , the maximum error observed was of $\pm 5\%$.

Comparison of numerical based results with laboratory tests

A considerable number of minor-axis joints laboratory tests have been performed at the University of Liège by Jaspart, Jaspart and Gomes, Ref [2], [6]. These included bolted and directly welded beams to the column web. In all these tests, set-up allowed the measurement of the deformation of the column web alone, thus giving us the possibility to compare results directly to our numerical models and proposals for the stiffness evaluation, and Gomes proposals for the plastic force or moment.

A good agreement was found when comparing $M-\phi$ numerical and experimental curves, validating our numerical model.

Figure 7c compares numerical simulations performed with LUSAS to laboratory tests of bolted connections, made by Jaspart and Gomes, Ref [2]. Test A12S is of a flange-cleat connection - mesh in Figure 7a, and Test A1 is of an end-plate connection - mesh in Figure 7b.

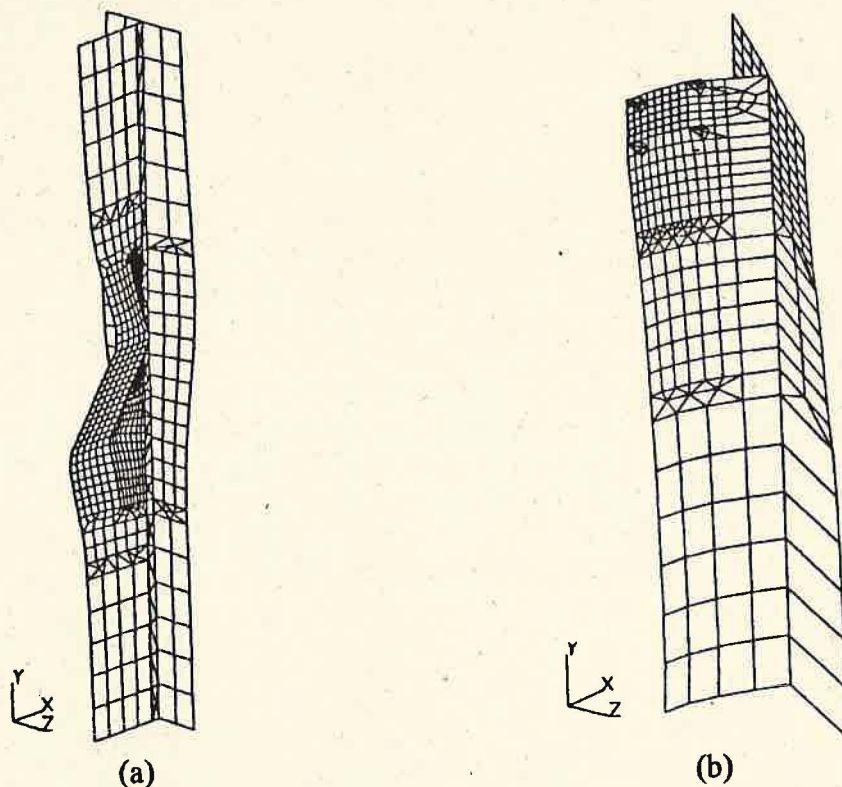


FIGURE 7 (a) and (b) - Mesh used for tests A12S and A1 respectively

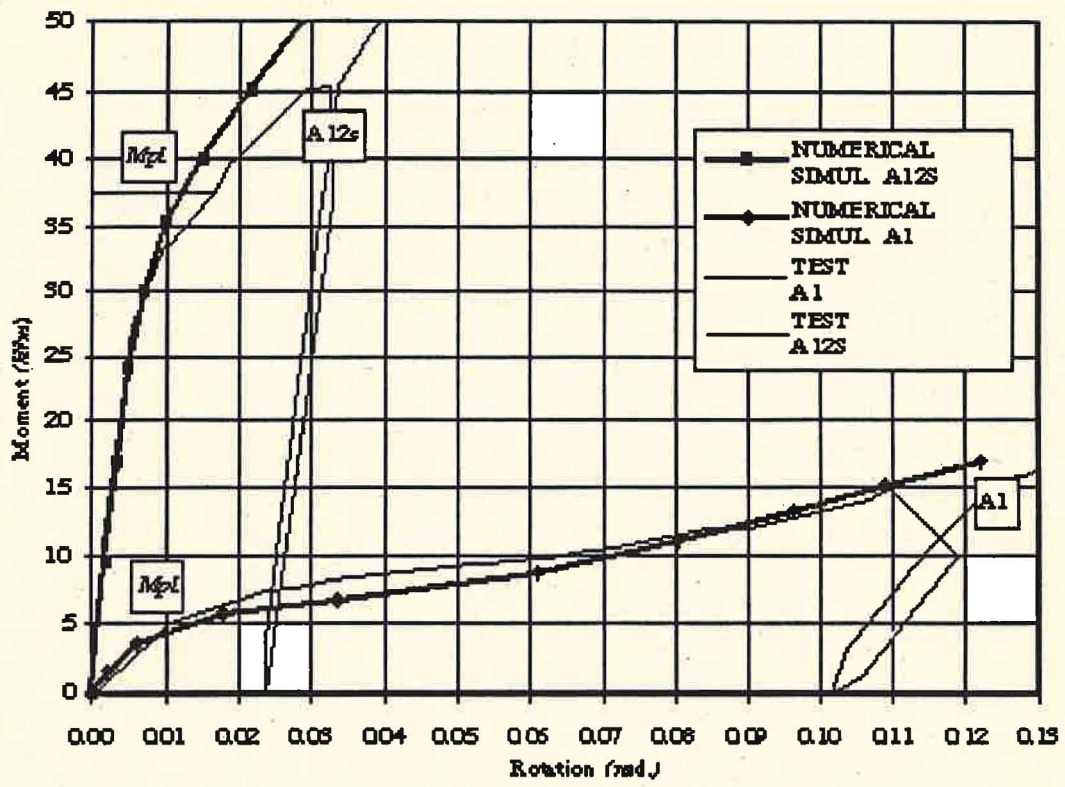


FIGURE 7 - Numerical simulations of Tests A1 and A12S [2]

Figure 8 is an example of a series of comparisons that we have made at the University of Liège, Ref [13], that were complementary to others, made by Jaspert et al, Ref [6]. The finite element package was FINELG and the tests, Ref [6], were performed on columns with beams directly connected to their webs by welding.

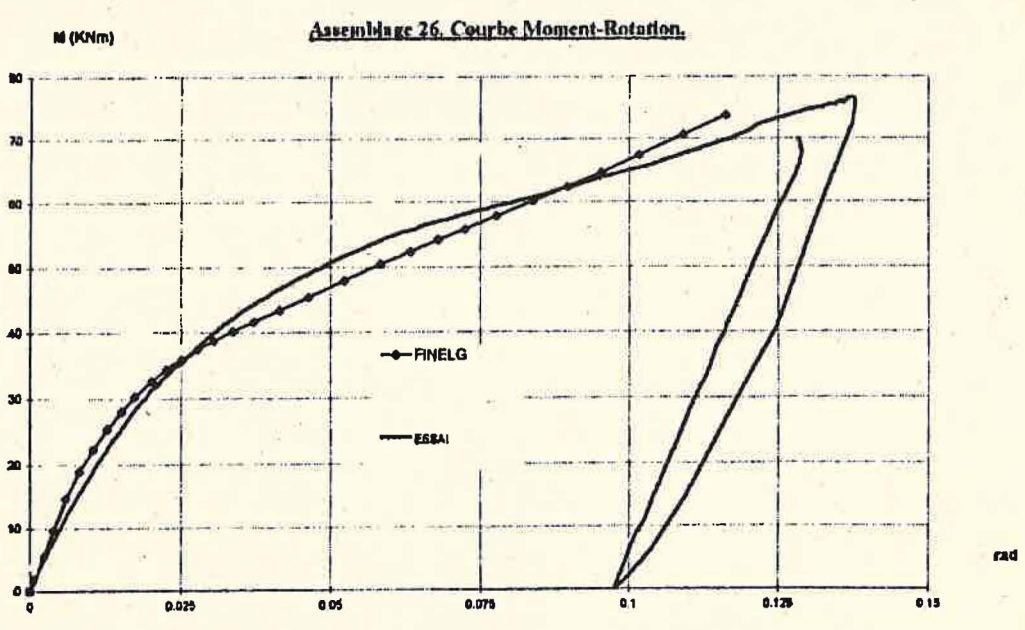


FIGURE 8 - Numerical simulation of a welded connection - test n° 21 [6]

CONCLUSIONS

Guidelines for the modelling of a column web in a minor-axis joint have been presented. Some of the most relevant conclusions are that thick shell elements may be used to model the column web and that a material and geometrical nonlinear analysis has to be performed in the general case. When modelling a tridimensional joint the column web may be considered as a plate clamped at the lines connecting it to the flanges, but in a minor-axis joint alone, flanges have to be modelled as well.

Reports from comparisons of laboratory tests to models calibrated with numerical simulations following these guidelines, show good results. A good correspondence was found as well when comparing some of these tests to our numerical simulations.

REFERENCES

- [1] - FEA, LUSAS 11.0 User Manual, FEA; UK.
- [2] - GOMES, F.C.T., Etat Limite Ultime de la Résistance de L'âme d'une Colonne dans un Assemblage Semi-Rigide d'axe Faible, Rapport Interne n° 203, MSM - Université de Liège, 1990, 72p.
- [3] - GOMES, F.C.T., JASPART, J.-P., Experimental research of minor-axis joints. Comparison with theoretical predictions, COST C1 WG2 Meeting, Coimbra, Nov. 1994. Doc. COST C1/WD2/94-13.
- [4] - GOMES, F.C.T., JASPART, J.P., MAQUOI, R., Behaviour of Minor Axis Joints and 3-D Joints, Proceedings of the second state-of-the-art workshop on Semi-Rigid Behaviour of Civil Engineering Structural Connections, Prague, Oct. 1994, pp. 111-120.
- [5] - GOMES, F.C.T., JASPART, J.P., Experimental Research of minor axis joints. Comparison with theoretical predictions. COST C1 - WG2 Meeting. Coimbra 25-26 Nov. 1994.
- [6] - JASPART, J. P., MAQUOI, R., GUISSÉ, S., LOGNARD, B., TAQUET, F., Sixième Rapport Semestriel Recherche COST C1, Septembre 1995, Université de Liège.
- [7] - KOROL, R., MIRZA, F., Finite Element Analysis of RHS T-Joints, Journal of the Structural Division, ASCE, vol.108, No. ST9, Sep.1982, pp 2081-2098.
- [8] - LU, L. H., PUTHLI, R.S., WARDENIER, J., Semi-Rigid Connections Between Plates and Rectangular Hollow Section Columns, Proceedings of the Fifth International Symposium on Tubular Connections held at Nottingham, UK, Aug. 1993, E & FN Spon, London, 1993, pp 723-731.

- [9] - NEVES, L.F.C., GOMES, F.C.T., Numerical simulation of a column web in a minor-axis joint, COST C1 WG6 Meeting, Trento-Itália, Junho 1995. Doc. COST C1/WG6/95-14.
- [10] - NEVES, L.F.C., GOMES, F.C.T., Parametric study on the behaviour of minor-axis joints, COST C1 WG2 Meeting, Coimbra, Nov. 1994. Doc. COST C1/WD2/94-14.
- [11] - NEVES, L.F.C., Semi-rigid connections in steel structures. Assessment of stiffness for minor-axis geometries. (In Portuguese), thesis submitted in partial fulfilment of the requirements for the degree of Master of Structures, Coimbra, 1996.
- [12] - NEVES, L.F.C., GOMES, F.C.T., Semi-rigid behaviour of beam-to-column minor-axis joints, Proceedings of the IABSE International Colloquium on Semi Rigid Structural Connections, Istanbul - Turkey, Sept. 1996.
- [13] - NEVES, L.F.C., Rapport final de Mission COST sur la semi-rigidité de noeuds poutre-colonne d'axe faible, Université de Liège, MSM, Décembre 1996.
- [14] - TING, L.C., SHANMUGAM, N.E., LEE, S.L., Box-Column to I-Beam Connections with External Stiffeners, J. Constructional Steel Research 18, 1991, pp 209-226.
- [15] - ZANG, Z., NIEMI, E., Studies of the Behaviour of RHS Gap K-Joints by Non-Linear FEM, Proceedings of the Fifth International Symposium on Tubular Connections held at Nottingham, UK, Aug. 1993, E & FN Spon, London, 1993, pp 364-372.

BENCHMARK EXPERIMENTS FOR NUMERICAL SIMULATIONS OF T-STUBS

N. Gebbeken & T. Wanzek

University of the Federal Armed Forces Munich, Germany

In this paper an overview of the Munich t-stub experiments will be given. These experiments have been carried out for the purpose of a comparison to numerical simulations. Therefore detailed material informations of the rolled section and the bolts had to be determined. For a valid comparison it was necessary to measure the static (rate independent) values of the material and of the experiment's loading. Additional to the usual deformation, bolt forces and strains were measured, so that a detailed comparison to numerical analyses is possible. The procedure of the t-stub experiments and of the material testing are described in this paper.

INTRODUCTION

The investigated specimen are the well known symmetrical t-stub connections. Up to now many t-stub experiments were carried out with the aim to develop design rules for end plate connections (e.g. Zoetemeijer [5]). The background of these investigations is the Eurocode 3 which allows the use of semi-rigid connections. Therefore, moment-rotation relationships, which represent the deformation capacity are required for frame analysis. In order to study the structural behaviour of connections very carefully, it is necessary to carry out extensive parametric studies. Some experiments on end plate connections have been carried out e.g. by Zoetemeijer [6] and Humer [2]. But experimental parametric studies are extremely time consuming and costly.

The idea was to accelerate developments by partly substituting experiments by finite element analyses, or to calculate the moment-rotation behaviour of a proposed connection directly. To achieve this, fundamental knowledge of finite element modelling is required. Therefore it was suggested to study first a t-stub connection as a benchmark problem. By doing this, it became clear that the provided experimental data, which should be used as finite element calculation input data were insufficient.

Therefore, we decided to carry out experiments in order to provide all necessary data that are required for finite element analyses. That means stress-strain relationship of the materials, static and dynamic values, and various force-deformation-relationships. This paper will give an overview of these experiments. The detailed informations can be found in the experimental report from Gebbeken, Wanzek and Petersen [1].

SPECIMEN

Dimension Size

Three types of specimen, which can basically be distinguished by different sizes and bolt distances, have been chosen. The member pieces were manufactured from one strand of a IPE 300 profile. One flange was cutted off at a height of 270 mm. 24 pieces are of $l=105$ mm length and 12 pieces are of $l=210$ mm length. Types 1 and 3 are manufactured from the shorter pieces. They are distinguished by the bolt distances e_2 perpendicular to the web (Figure 1). The characteristic measures are given in Table 1 and the actual measures are listed in the report [1].

Material Data – Profile

The entire stress-strain relationship is required as input data for numerical analysis. For this sake, four standard tension test specimen are manufactured out of the steel member as shown in Figure 2. Strain gages were applied on both sides positioned in the middle of the characteristic length. The available strain gages were only valid in the elastic range. Therefore, an extensometer that measured over a distance of 25 mm was also used. Due to the measuring range of ± 2.5 mm we were only be able to record up to 10 % strain. But actually, the standard tension test specimen failed at $\varepsilon_u = 29.5$ % strain.

In order to compare different tests and for the sake of numerical simulation it was necessary to determine the static stresses. This is of importance because the stresses, especially in the plastic regime are rate-dependent. Static stresses are defined as such stresses that are obtained during a hold on of the deformation driven experiment. It was observed that the static stresses were reached after a period of approximately one minute. The total hold on lasted for three minutes. It was already known that the value of stress reduction is nearly independent of the amount of strain (Petersen [3]; Scheer, Maier und Rohde [4]). Our own tests confirmed this, and consequently, it was easy to determine the static stress-strain curve (Figure 3). The stress reduction was approximately 20 N/mm².

Table 2.2 provides the characteristic data of the tension tests and the data taken over from the German Standard.

Material Data – Bolt

All used high-strength bolts, M16, grade 10.9 according to DIN 6914, belonged to the same charge. With the help of an especially constructed testing device (Figure 4a) we determined characteristic bolt-elongation curves as well as the failure load. For these experiments the bolts were only tightened by hand. The strains at the bolt shank were measured using two opposite strain gages (Figure 4b). The two obtained load-strain curves were averaged and the Young's modulus was calculated. The characteristic Young's modulus was determined with the help of a linear regression analysis of the strain-force curve in several ranges and resulted in 214000 N/mm².

With the provided Young's modulus the bolt forces can be calculated from the strain measurement at the bolts during the t-stub experiments. The bolt-elongation curve is necessary for the calibration of the bolts in a finite element model.

TESTING PROCEDURE

We carried out two series with three specimen each for each testing type. One series was performed with hand-tightened bolts and one with prestressed bolts. The indication of the tests are listed in Table 3. The bolts of the "hand-tightened" specimen were fastened by using an ordinary spanner yielding a pretension of about 30 *kN*. The fully prestressed bolts were fastened applying a torque wrench spanner (prestressed with 260 *Nm*) yielding in a bolt force of about 100 *kN*.

Chronological Plan

The description of the testing procedure in this subsection starts at the point when the specimen were totally assembled and the bolts were only tightened by hand. From this point on, all extensometers and strain gages were already in operation.

Phase 1: Before installing into the testing machine

- Start of electronic recording
- Tightening of the bolts

Phase 2: Installation of the specimen into the testing machine

Phase 3: Start: Force driven

- Force driven test up to test load of $F=60 \text{ kN}$
- Hold on of the tests in order to measure the length of the bolts

Phase 4: Start: Displacement driven and stops

- Displacement driven test starts at $F=60 \text{ kN}$
- Hold on of the test in order to measure the length of the bolts

Static Load

The static load is one of the very important properties of an experiment. The static load ensures the comparison with other experiments and with numerical simulations, because it provides test speed independent results. In order to achieve the static load, the t-stub tests were interrupted temporarily similar to the static stress (Figure 5). The force-drop during the hold on was about 15 *kN* and took mainly place in the first 60 seconds. After three minutes the further drop was negligible. So, the interruption period was chosen to be three minutes.

Measurement of the Gap

A characteristic and well defined deformation of the T-Stub is the gap of the flanges measured in the centerline of the webs. This deformation can be compared with other test results which were carried out with other machines, because the gap is not affected by the elasticity of the machine, clamped conditions etc. Here the gap was measured at opposite sides of the specimen as shown in Figure 7. For technical reasons, the extensometers were fastened at the web in a distance of 40 *mm* from the bottom of the flange. Therefore not the pure gap was measured; a little portion of the deformation of the profile is part of the „measured gap“. But, this portion is maximal 2% of the measured gap and can be neglected. This has been determined by numerical simulations.

The differences between the measured gaps of both sides were small, therefore, the average of these values was taken for the diagrams. While tightening the bolts negative gap values (0.45 – 0.60 mm) have been recorded. They represent the geometrical imperfections of the flanges.

Measurements at the Bolts

In order to determine the bolt force, strains at the shank as well as bolt elongation were recorded. The strain measurement was the same as carried out for the bolt tests; two strain gages at opposite side (Figure 4b). The bolts were assembled in such a way that the line of the strain gages was perpendicular to the web. In order to determine the normal force and the bending moment of the bolt, a linear strain distribution from one strain gage to the other was assumed.

The scattering of the bolt forces after pretension usually was about 10 kN, only in three experiments one bolt had a quite different pretension force. The scattering of the bolt forces of each series (two experiments) was about 10 – 15 kN. Even the bolt forces of the same experiment can differ in the same way as the pretension forces were different (Figure 6). Nevertheless, the bolt forces can be seen as reliable, because the scattering is small. In contrast to the forces, the bolt moments scatter too much and have to be used carefully (Figure 6).

Because of cost restrictions not all bolts could be applied with strain gages. In addition, some strain gages failed after coming into contact with the inner edge of the bolt hole. In order to overcome these deficiencies a special bolt elongation measurement device has been developed. But the elongation measurement was too sensitive and not precise enough to calculate reliable bolt forces.

Profile Strains

Our main interest was to compare measured strains with numerical strains obtained by the finite element simulation. This is a much more severe test than just comparing forces and deformations. So, strain gages were applied at the upper flanges of two out of three specimen of one series (Figure 7). And in addition strain gages were applied at the web on opposite sides to record a possible web moment.

While installing and clamping the specimen it could be observed that bending in the webs occur. The values of the bending moments raised while running the test as long as the load-deflection characteristic was quasi linear. We expected such bending moments caused by imperfections. However, there was no relation between the measured imperfections in the web and the values of the bending moments.

CONCLUDING REMARKS

The corresponding results of the three tests of one series deviate only a little. Because of the excellent coincidence of the deformation behaviour we can say that they are very reliable. The scattering of the measured strains is very small and that of the bolt forces is acceptable. But nevertheless, it is recommended to use these results by considering the whole range of the measured data of bolt or strains, respectively, in case the standard deviation is too large.

The experiments provide the necessary data and informations for finite element modelling in order to simulate these experiments. Again, we underline the importance of the determination of the static load and of the entire static stress-strain behaviour of the material. Only these informations make it possible to correctly perform numerical simulations referring to a rate-independent material law. It is self-evident, that detailed informations about the measurements on the testing procedure have to be given as well.

REFERENCES

- [1] Gebbeken, N., Wanzek, T., Petersen, C.: Semi-Rigid Connections, T-Stub Modelle – Versuchsbericht –, Report on Experimental Investigations. Berichte aus dem Konstruktiven Ingenieurbau der Universität der Bundeswehr München, Nr. 97/2, ISSN 1431-1522 (1997)
- [2] Humer, C.: Das Momenten-Rotationsverhalten von steifenlosen Rahmenknoten mit Kopfplattenanschlüssen, Dissertation, Universität Innsbruck, Institut für Stahlbau und Holzbau, 1987
- [3] Petersen, C.: Stahlbau, Braunschweig Wiesbaden, Vieweg, 1997
- [4] J. Scheer, W. Maier, M. Rohde: Zur Qualitätssicherung mechanischer Eigenschaften von Baustahl, Bericht 6087/1, Technische Universität Braunschweig, Institut für Stahlbau, 1987
- [5] Zoetemeijer, P.: A Design Method for the Tension Side of Statically Loaded Bolted Beam-to-Column Connection. Heron, Vol. 20, Technische Hogeschool Delft, 1974
- [6] Zoetemeijer, P.: A Design Method for Bolted Beam-to-Column Connections with Flush End-Plates and Haunched Beams. Stevin Report Nr. 6-82-7, Technische Hogeschool Delft, 1982
- [7] Zoetemeijer, P., Munter, H.: Proposal for the Standardization of Extended End-Plate Connections Based on Test Results. Stevin Report Nr. 6-83-23, Technische Hogeschool Delft, Dezember 1983

Tables and Figures

- Table 1: Dimension size of each specimen type (denotation see Figure 1).
- Table 2: Characteristics of the tension tests.
- Table 3: Denotation of t-stub experiments.
- Figure 1: Denotation of the geometrical measurement of the profiles.
- Figure 2: Test Specimen of the Tensile Tests.
- Figure 3: Measured and static stress-strain curve. Test specimen belongs to web transverse to direction of rolling
- Figure 4: (a) Testing device to achieve the bolt characteristic.
(b) Strain gages at the bolt in the bolt test as well as in the t-stub experiments.
- Figure 5: Experiment P1K. Deformation characteristic presented by the gap-load curve including the static values.
- Figure 6: Experiment P1K. Bolt forces and bolt moments.
- Figure 7: Gap measurement and position of the strain gages.

| | | Pos. 1 | Pos. 2 | Pos. 3 |
|------------------|----------------|--------|--------|--------|
| width | b | 150,0 | | |
| flange thickness | t | 10,7 | | |
| web thickness | s | 7,1 | | |
| profile length | l | 105,0 | 210,0 | 105,0 |
| hole positions | p ₁ | 55,0 | 90,0 | 55,0 |
| along web | p ₂ | 25,0 | 60,0 | 25,0 |
| hole positions | e ₁ | 100,0 | 100,0 | 90,0 |
| perp. to web | e ₂ | 25,0 | 25,0 | 30,0 |

Table 1:

| | | nominal values Fe360 t < 16mm | flange parallel to web | flange perp. to web | web |
|--------------------------|-------------------|-------------------------------------|---------------------------|------------------------|-----------------|
| upper elastic limit | N/mm ² | 235 | 304 | 290-300 | 343 |
| lower elastic limit | N/mm ² | | 296 - 288 | 280 | 300 - 310 |
| tensile strength | N/mm ² | 340 - 370 | 422 | 435 | 425 / 440 |
| failure elongation | % | 26 | 29 | 30 | 26 / 30 |
| transverse elongation | % | | 65 | 65 | 59 / 67 |
| Young's modulus | N/mm ² | 210000 | 203600 | 206500 | 202200 / 208900 |

Table 2:

| | „no“ pretension | | full pretension | |
|-----------------|-------------------------------------|-------|-------------------------------------|-------|
| | strain gages at flange and bolts | | strain gages at flange and bolts | |
| specimen type 1 | P1K-1 P1K-2 | P1K-3 | P1V-1 P1V-2 | P1V-3 |
| specimen type 2 | P2K-1 P2K-2 | P2K-3 | P2V-1 P2V-2 | P2V-3 |
| specimen type 3 | P3K-1 P3K-2 | P3K-3 | P3V-1 P3V-2 | P3V-3 |

Table 3:

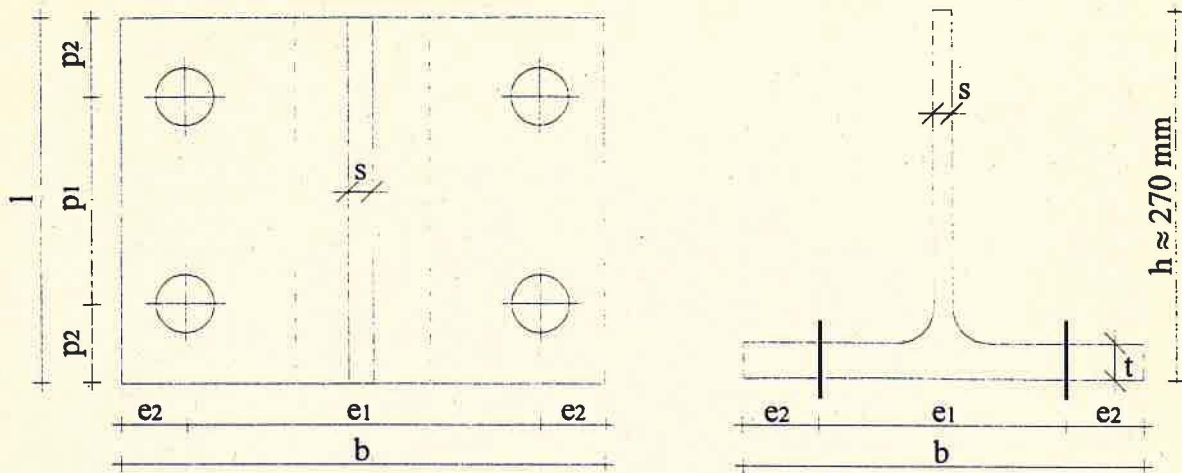


Figure 1:

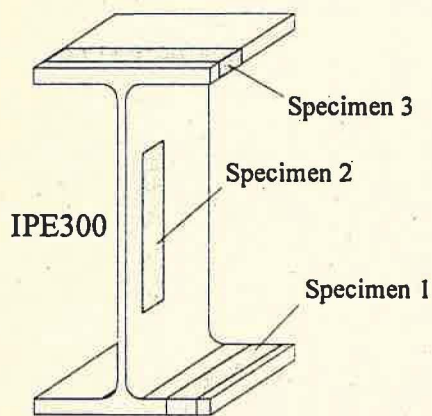


Figure 2:

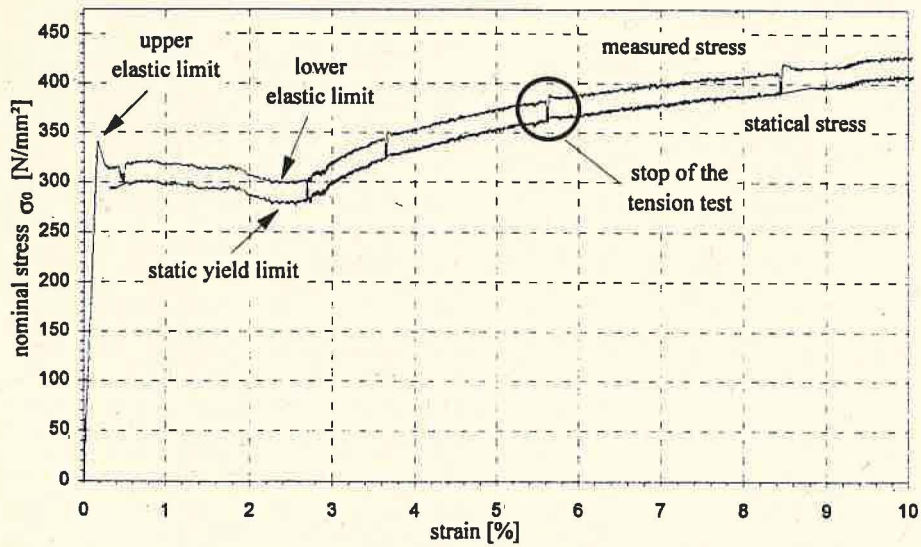


Figure 3:

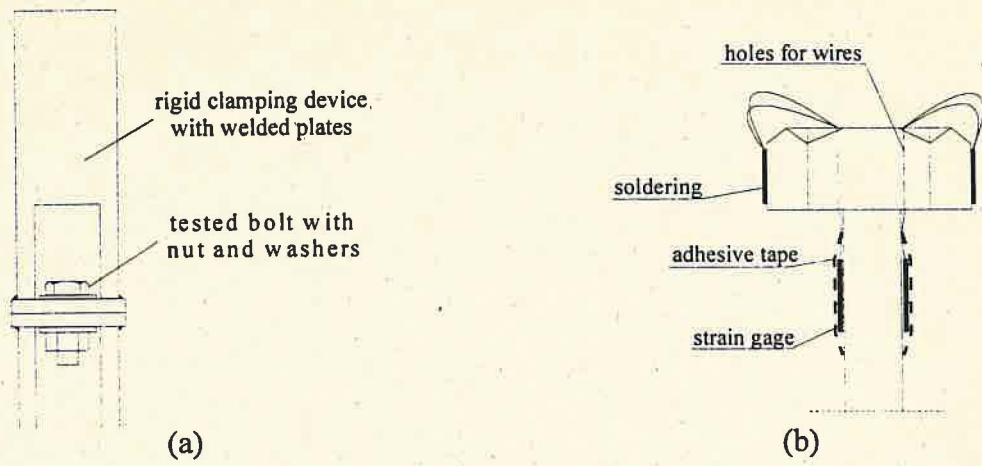


Figure 4:

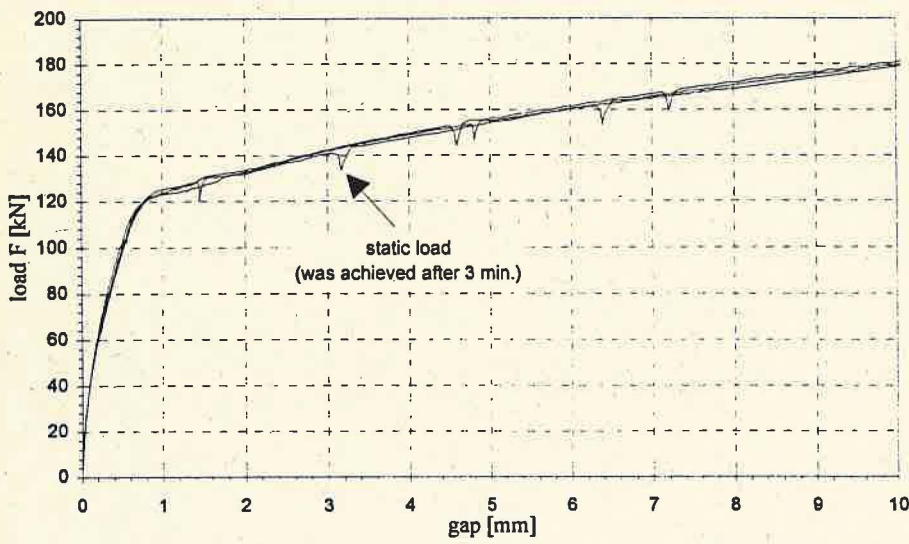


Figure 5:

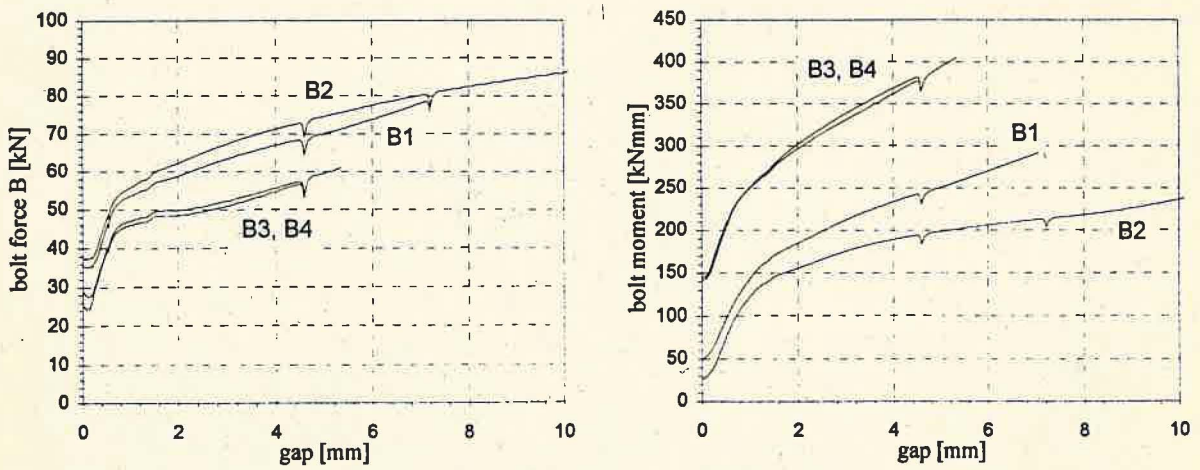


Figure 6:

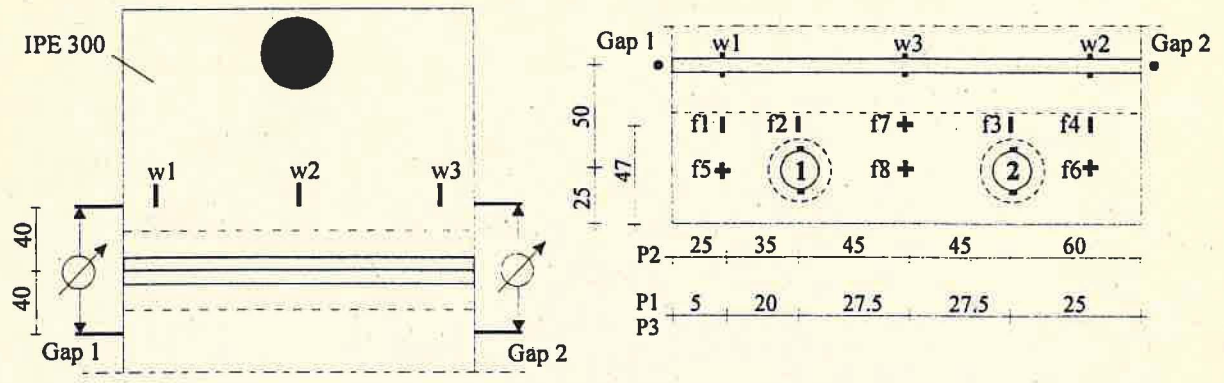


Figure 7:

CONTACT ADDRESSES

Dr František WALD
Department of Steel Structures
Faculty of Civil Engineering
Czech Technical University
Thákurova 7
CZ-166 29 - PRAHA 6
Czech Republic

Telephone: +42 2 2435 4757
Telefax: +42 2 311 7466
or +42 2 311 7034
E-mail: wald@fsv.cvut.cz

Prof Dr Ing N GEBBEKEN
Fakultät für Bauingenieur- und Vermessungswesen
Institut für Mechanik und Statik
Universität der Bundeswehr München
Werner Heisenberg Weg 39
D-85579 NEUBIBERG
Germany

Telephone: +49 89 60 04 32 39
Telefax: +49 89 60 04 35 60
E-mail: norbert.gebbeken@unibw-
muenchen.de

Dr Ing C C BANIOPOULOS
Institute of Steel Structures
School of Technology
Aristotle University
GR-54006 THESSALONIKI
Greece

Telephone: +30 31 99 57 53
Telefax: +30 31 99 56 42
E-mail: iss@heron.civil.auth.gr

Dr Luis NEVES
Department of Civil Engineering
University of Coimbra
P-3049 COIMBRA Cedex
Portugal

Telephone: +351 39 410 676/697
Telefax: +351 39 22 833
E-mail: lfneves@ci.uc.pt

Prof K S Viridi
Department of Civil Engineering
City University
Northampton Square
LONDON EC1V 0HB
UK

Telephone: +44 171 477 8142
Telefax: +44 171 477 8570
E-mail: k.s.virdi@city.ac.uk